Part III

Equations of Motion

Chapter 6

Equations of motion (barotropic component)

Historically, iterative methods have been used to solve the barotropic part of the momentum equations by applying the rigid-lid approximation. The number of iterations to get convergence of a solution is of order N, where N is the larger number of grid points of the two horizontal directions. Thus the number of iterations increases as the number of grid points increases. This means that the iterative process could occupy a large part of the total CPU time. This is a severe burden and should be remedied.

An alternative is to replace the rigid lid with a free surface. The number of short barotropic time steps within a long baroclinic time step is roughly decided by the ratio between external and internal gravity wave speeds, around 70 to 100, which becomes smaller than N when the number of grid points of the model is large.* In addition, this method is more suitable for parallel computation than the iterative methods. Thus, for fine-resolution models, the free-surface formulation has numerous advantages over the iterative methods. The free-surface formulation was adopted in the Bryan-Cox-Semtner numerical ocean general circulation models by Killworth et al. (1991).

However, the free-surface formulation has a problem when it is used with a mixed-layer model. To appropriately resolve the surface mixed layer, the uppermost layer should be less than a few meters thick. This leads to a serious problem, since a free-surface model does not work when the sea surface is below the bottom of the uppermost layer and the thickness of this layer vanishes. This occurs in world ocean models, because the difference between the maximum and minimum of the sea surface height becomes several meters.†

To remedy this problem, σ-coordinate has been adopted near the sea surface until MRI.COM version 3. This method is called σ-z formulation and is introduced by Hasumi (2006). The thicknesses of the several upper layers ($z \leq -H_B$) vary as the sea surface height does whereas the vertical position of the layers below ($z = -H_B$) is kept fixed (Figure 6.1a).

There were two major shortcomings in the implementation of the σ-z formulation in MRI.COM. First, because we set H_B as a constant, the sea-floor cannot be shallower than H_B. We typically take H_B as 20 - 30 meters, thus the representation of circulation around coastal areas with shallow sea-floor may not be accurate. Second, because a hybrid of vertical coordinates is used, some sort of dynamical analyses may be awkward.

To resolve these problems, a vertically rescaled height coordinate (z^*) introduced by Adcroft and Campin (2004), where undulation of the sea surface is distributed to all vertical grid cells in a water column, is adopted in MRI.COM version 4.

In this chapter, we explain the free-surface formulation of MRI.COM with z^* vertical coordinate.

6.1 Governing equations

As described in Chapter 2, the prognostic variables in the free-surface model are the surface elevation (η) and the vertically integrated velocity (U and V). The prognostic equations are obtained by integrating momentum and continuity equations vertically.

The momentum equations (2.69) and (2.70) are re-written:

$$\frac{\partial U}{\partial t} - fV = -\frac{(\eta + H)}{\rho_0 h_\mu}\frac{\partial(p_a + \rho_0 g\eta)}{\partial \mu} + X, \tag{6.1}$$

$$\frac{\partial V}{\partial t} + fU = -\frac{(\eta + H)}{\rho_0 h_\psi}\frac{\partial(p_a + \rho_0 g\eta)}{\partial \psi} + Y, \tag{6.2}$$

* A North Pacific model with $1/4° \times 1/6°$ resolution, which was the first meso-scale eddy permitting model developed by the ocean modeling group of MRI about 20 years ago, had 742 grid points in the zonal direction. This figure prompted us to make a transition from the rigid-lid to free surface formulation.

† For example, the maximum and minimum sea-surface heights in a $1° \times 1°$ world ocean model are about 1 m (subtropical gyres) and -2 m (the Ross Sea), respectively.

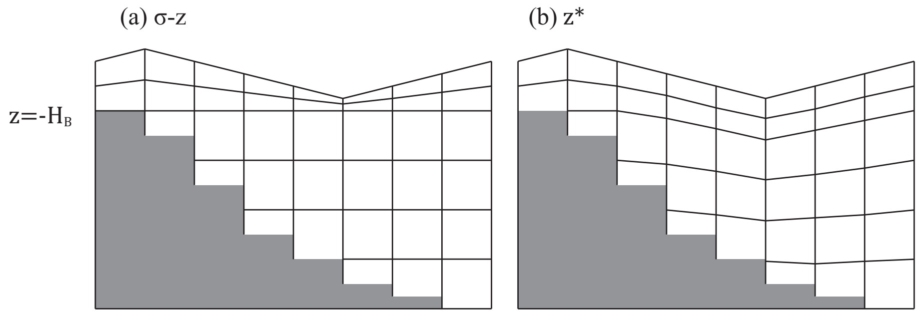

Figure6.1 Schematic of (a) the near surface σ-coordinate layers (σ-z coordinate) and (b) z^* vertical coordinate.

where

$$X \equiv \sum_{k=1}^{N} F_\mu = -\nabla_H \cdot \Big(\sum_{k=1}^{N}(\Delta z(u,\ v)u)_{k-\frac{1}{2}}\Big) - \sum_{k=1}^{N}\Big[\frac{v}{h_\mu h_\psi}\left(\frac{\partial h_\mu}{\partial \psi}u - \frac{\partial h_\psi}{\partial \mu}v\right)\Big]_{k-\frac{1}{2}}\Delta z_{k-\frac{1}{2}}$$
$$- \sum_{k=1}^{N}\Big[\frac{1}{\rho_0}\frac{1}{h_\mu}\int_{s_{k-\frac{1}{2}}}^{0} z_s g \rho_\mu ds'\Big]\Delta z_{k-\frac{1}{2}} - \frac{g}{\rho_0 h_\mu}\sum_{k=1}^{N}[\rho' z_\mu]\Delta z_{k-\frac{1}{2}} + \sum_{k=1}^{N}(\Delta z F^{\mu}_{\text{horz}})_{k-\frac{1}{2}} + F^{\mu}_{\text{surf}}\Delta z_{\frac{1}{2}} + F^{\mu}_{\text{bottom}}\Delta z_{N-\frac{1}{2}} \tag{6.3}$$

$$Y \equiv \sum_{k=1}^{N} F_\psi = -\nabla_H \cdot \Big(\sum_{k=1}^{N}(\Delta z(u,\ v)v)_{k-\frac{1}{2}}\Big) + \sum_{k=1}^{N}\Big[\frac{u}{h_\mu h_\psi}\left(\frac{\partial h_\mu}{\partial \psi}u - \frac{\partial h_\psi}{\partial \mu}v\right)\Big]_{k-\frac{1}{2}}\Delta z_{k-\frac{1}{2}}$$
$$- \sum_{k=1}^{N}\Big[\frac{1}{\rho_0}\frac{1}{h_\psi}\int_{s_{k-\frac{1}{2}}}^{0} z_s g \rho_\psi ds'\Big]\Delta z_{k-\frac{1}{2}} - \frac{g}{\rho_0 h_\psi}\sum_{k=1}^{N}[\rho' z_\psi]\Delta z_{k-\frac{1}{2}} + \sum_{k=1}^{N}(\Delta z F^{\psi}_{\text{horz}})_{k-\frac{1}{2}} + F^{\psi}_{\text{surf}}\Delta z_{\frac{1}{2}} + F^{\psi}_{\text{bottom}}\Delta z_{N-\frac{1}{2}}. \tag{6.4}$$

Note that the surface atmospheric pressure p_a is omitted in the remainder of this chapter. In MRI.COM, the surface atmospheric pressure is not included unless explicitly specified by SLP option.

The continuity equation (2.73) is re-written:

$$\frac{\partial \eta}{\partial t} + \frac{1}{h_\mu h_\psi}\left\{\frac{\partial (h_\psi U)}{\partial \mu} + \frac{\partial (h_\mu V)}{\partial \psi}\right\} = (P - E + R + I), \tag{6.5}$$

where P is precipitation (positive downward), E is evaporation (positive upward), R is the river discharge rate (positive into the ocean), and I is the mass exchange with the sea ice model (positive into the ocean).

Figure 6.2 illustrates the grid arrangement of the free-surface formulation. The variable η is defined at T-points, and the variables U and V are defined at U-points. Forcing terms (X and Y) in Eqs. (6.1) and (6.2) are calculated in the subroutine for the baroclinic component and defined at U-points.

6.2 Time integration on barotropic time levels

Figure 6.3 presents schematics of the time integration of the barotropic mode in the free-surface formulation. When the time integration of the baroclinic mode is performed from step n ($t = t_n$) to step $n + 1$ ($t = t_{n+1}$, $\Delta t = t_{n+1} - t_n$), the corresponding time integration of the barotropic mode is carried out from step n to a step sometime beyond step $n + 2$ with the barotropic time interval Δt_{tr} using the vertically integrated values (X, Y) at $t = t_n$ calculated in the program that solves the baroclinic mode. A weighted average of the barotropic mode over the integration period is used to represent the vertically integrated velocity at $t = t_{n+1}$.

The "Euler forward-backward" scheme is a stable and economical numerical scheme for linear gravity wave equations without advection terms (Mesinger and Arakawa, 1976), and this is adopted for the governing equations in the free-surface formulation of MRI.COM. This scheme is more stable than the leap-frog scheme. The time step can be doubled for

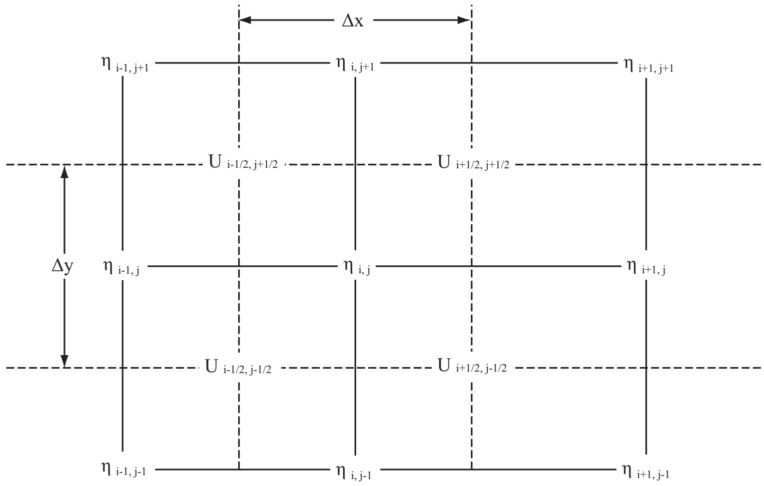

Figure6.2 Grid arrangement of the free-surface formulation

the linear gravity wave equations. In this numerical scheme, either the continuity equation or the momentum equation is calculated first, and then the estimated values are used for calculating the remaining equations. In the procedure of MRI.COM, the surface elevation is first calculated using the continuity equation; the calculated surface elevation is then used to calculate the pressure gradient terms of the momentum equations.

Killworth et al. (1991) recommended using the Euler backward (Matsuno) scheme for the free surface model except for the tidal problem. The Euler-backward scheme damps higher modes and is more stable. However, the computer burden increases considerably because this scheme calculates the equations twice for one time step. In MRI.COM, stable solutions are efficiently obtained by using the Euler forward-backward scheme because the time filter is applied for the barotropic mode.

The finite-difference expression of the continuity equation (Eq. 6.5) is

$$\frac{(\eta'_{i,j} - \eta_{i,j})}{\Delta t_{\mathrm{tr}}} + \frac{1}{(h_\mu h_\psi)_{i,j}} \left[(\delta_\mu \overline{h_\psi U}^{\psi})_{i,j} + (\delta_\psi \overline{h_\mu V}^{\mu})_{i,j} \right] = (P - E + R + I)_{i,j}, \tag{6.6}$$

where the subscripts are labeled on the basis of T-points. The variable $\eta_{i,j}$ is located at T-points, and the variables $U_{i+\frac{1}{2},j+\frac{1}{2}}$ and $V_{i+\frac{1}{2},j+\frac{1}{2}}$ are located at U-points. (They are located at $(i + \frac{1}{2}, j + \frac{1}{2})$ on the basis of T-points; see Figure 3.3). The finite-differencing and averaging operators are defined as follows:

$$\begin{aligned} \delta_\mu A_i &\equiv \frac{A_{i+\frac{1}{2}} - A_{i-\frac{1}{2}}}{\Delta\mu_i}, & \delta_\mu A_{i+\frac{1}{2}} &\equiv \frac{A_{i+1} - A_i}{\Delta\mu_{i+\frac{1}{2}}}, \\ \overline{A_i}^{\mu} &\equiv \frac{A_{i+\frac{1}{2}} + A_{i-\frac{1}{2}}}{2}, & \overline{A_{i+\frac{1}{2}}}^{\mu} &\equiv \frac{A_{i+1} + A_i}{2}. \end{aligned} \tag{6.7}$$

The same applies to ψ. In the program codes, the above equation is multiplied by the area of a T-cell ($\Delta S_{T\,i,j} = (\Delta x \Delta y)_{i,j} = (h_\mu \Delta\mu h_\psi \Delta\psi)_{i,j}$):

$$\begin{aligned} &(\eta'_{i,j} - \eta_{i,j}) \cdot \Delta S_{T\,i,j} \\ &\quad = \Delta t_{\mathrm{tr}} \cdot \left\{ (P - E + R + I)_{i,j} \cdot \Delta S_{T\,i,j} - \left(\Delta y_{i+\frac{1}{2},j} \overline{U}^{\psi}_{i+\frac{1}{2},j} - \Delta y_{i-\frac{1}{2},j} \overline{U}^{\psi}_{i-\frac{1}{2},j} \right) - \left(\Delta x_{i,j+\frac{1}{2}} \overline{V}^{\mu}_{i,j+\frac{1}{2}} - \Delta x_{i,j-\frac{1}{2}} \overline{V}^{\mu}_{i,j-\frac{1}{2}} \right) \right\}. \end{aligned} \tag{6.8}$$

Averaging operators are defined the same way as the previous ones. This equation is used to obtain the new surface elevation, $\eta'_{i,j}$.

After obtaining $\eta'_{i,j}$, the momentum equations, Eqs. (6.1) and (6.2), are solved. A longer time step can be used when the semi-implicit scheme is applied for the Coriolis terms in the momentum equations. Their finite-difference forms are

$$\frac{(U'_{i+\frac{1}{2},j+\frac{1}{2}} - U_{i+\frac{1}{2},j+\frac{1}{2}})}{\Delta t_{\mathrm{tr}}} - \frac{f(V'_{i+\frac{1}{2},j+\frac{1}{2}} + V_{i+\frac{1}{2},j+\frac{1}{2}})}{2} = -\frac{g(H_{i+\frac{1}{2},j+\frac{1}{2}} + \overline{\overline{\eta'}}^{\mu,\psi}_{i+\frac{1}{2},j+\frac{1}{2}})}{(h_\mu)_{i+\frac{1}{2},j+\frac{1}{2}}} \delta_\mu \overline{\eta'}^{\psi}_{i+\frac{1}{2},j+\frac{1}{2}} + X_{i+\frac{1}{2},j+\frac{1}{2}} \tag{6.9}$$

$$\frac{(V'_{i+\frac{1}{2},j+\frac{1}{2}} - V_{i+\frac{1}{2},j+\frac{1}{2}})}{\Delta t_{\mathrm{tr}}} + \frac{f(U'_{i+\frac{1}{2},j+\frac{1}{2}} + U_{i+\frac{1}{2},j+\frac{1}{2}})}{2} = -\frac{g(H_{i+\frac{1}{2},j+\frac{1}{2}} + \overline{\overline{\eta'}}^{\mu,\psi}_{i+\frac{1}{2},j+\frac{1}{2}})}{(h_\psi)_{i+\frac{1}{2},j+\frac{1}{2}}} \delta_\psi \overline{\eta'}^{\mu}_{i+\frac{1}{2},j+\frac{1}{2}} + Y_{i+\frac{1}{2},j+\frac{1}{2}}. \tag{6.10}$$

Next, we solve these equations for $U'_{i+\frac{1}{2},j+\frac{1}{2}}$ and $V'_{i+\frac{1}{2},j+\frac{1}{2}}$. Let the r.h.s. of the above equations be GX and GY. Multiplying both sides by Δt_{tr}, we have

$$(U'_{i+\frac{1}{2},j+\frac{1}{2}} - U_{i+\frac{1}{2},j+\frac{1}{2}}) - \frac{f\Delta t_{\mathrm{tr}}}{2}(V'_{i+\frac{1}{2},j+\frac{1}{2}} + V_{i+\frac{1}{2},j+\frac{1}{2}}) = \Delta t_{\mathrm{tr}} GX_{i+\frac{1}{2},j+\frac{1}{2}}, \tag{6.11}$$

$$(V'_{i+\frac{1}{2},j+\frac{1}{2}} - V_{i+\frac{1}{2},j+\frac{1}{2}}) + \frac{f\Delta t_{\mathrm{tr}}}{2}(U'_{i+\frac{1}{2},j+\frac{1}{2}} + U_{i+\frac{1}{2},j+\frac{1}{2}}) = \Delta t_{\mathrm{tr}} GY_{i+\frac{1}{2},j+\frac{1}{2}}, \tag{6.12}$$

leading to

$$U'_{i+\frac{1}{2},j+\frac{1}{2}} - \frac{f\Delta t_{\mathrm{tr}}}{2} V'_{i+\frac{1}{2},j+\frac{1}{2}} = U_{i+\frac{1}{2},j+\frac{1}{2}} + \frac{f\Delta t_{\mathrm{tr}}}{2} V_{i+\frac{1}{2},j+\frac{1}{2}} + \Delta t_{\mathrm{tr}} GX_{i+\frac{1}{2},j+\frac{1}{2}}, \tag{6.13}$$

$$V'_{i+\frac{1}{2},j+\frac{1}{2}} + \frac{f\Delta t_{\mathrm{tr}}}{2} U'_{i+\frac{1}{2},j+\frac{1}{2}} = V_{i+\frac{1}{2},j+\frac{1}{2}} - \frac{f\Delta t_{\mathrm{tr}}}{2} U_{i+\frac{1}{2},j+\frac{1}{2}} + \Delta t_{\mathrm{tr}} GY_{i+\frac{1}{2},j+\frac{1}{2}}. \tag{6.14}$$

Letting the r.h.s. of the above equations be RX and RY, we may derive expressions for $U'_{i+\frac{1}{2},j+\frac{1}{2}}$ and $V'_{i+\frac{1}{2},j+\frac{1}{2}}$ as follows:

$$U'_{i+\frac{1}{2},j+\frac{1}{2}} = \left\{RX_{i+\frac{1}{2},j+\frac{1}{2}} + \frac{f\Delta t_{\mathrm{tr}}}{2} RY_{i+\frac{1}{2},j+\frac{1}{2}}\right\} \Big/ \left\{1 + \left(\frac{f\Delta t_{\mathrm{tr}}}{2}\right)^2\right\}, \tag{6.15}$$

$$V'_{i+\frac{1}{2},j+\frac{1}{2}} = \left\{RY_{i+\frac{1}{2},j+\frac{1}{2}} - \frac{f\Delta t_{\mathrm{tr}}}{2} RX_{i+\frac{1}{2},j+\frac{1}{2}}\right\} \Big/ \left\{1 + \left(\frac{f\Delta t_{\mathrm{tr}}}{2}\right)^2\right\}. \tag{6.16}$$

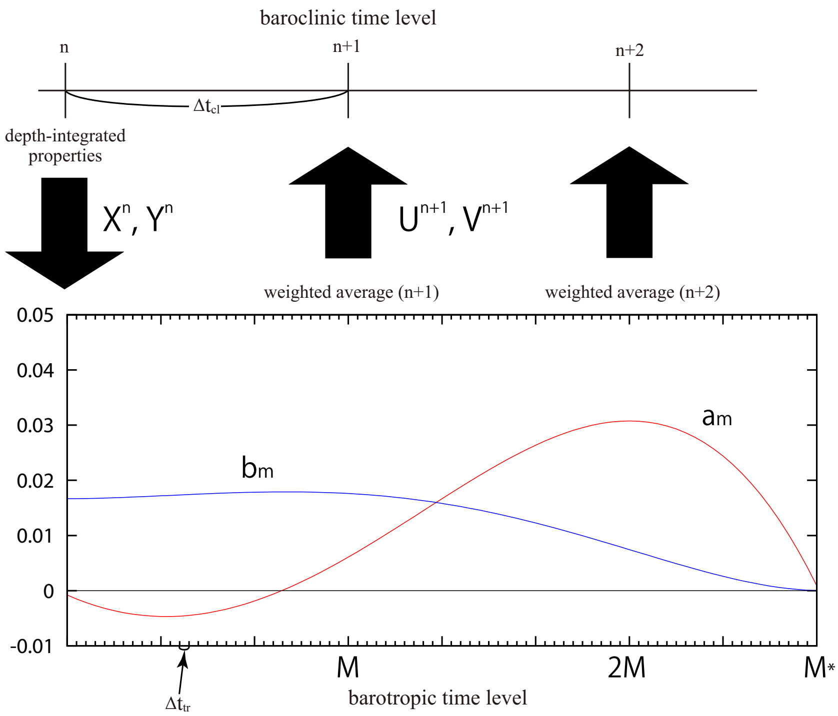

Figure6.3 Schematic figure of the time integration of the barotropic mode and its time-filtering procedure. a_m and b_m are weights for $t = n + 2$ and $t = n + 1$, respectively.

6.3 Prognostication of state variables at the baroclinic time level

In the split-explicit method, the state at the next baroclinic time level is obtained by using the solution of the barotropic mode explained in the previous section. To do this, an appropriate time-filtering is necessary. The velocity at the baroclinic time level uses the time-filtered barotropic state as the depth averaged velocity.

6.3.1 Weighted averaging to obtain a barotropic state at the baroclinic time level

The main purpose of solving the barotropic submodel on proceeding from the baroclinic time level of $t = t_n$ to $t = t_{n+1}$ is to obtain the barotropic state variables η, U, and V at the baroclinic time level of $t = t_{n+1}$. To achieve this, starting from the baroclinic time level of $t = t_n$, the governing equations of the barotropic submodel are integrated slightly beyond $t = t_{n+2}$ to compute the barotropic state variables as a weighted average of those at barotropic time levels.

We follow the method adopted by the Regional Oceanic Modeling System (ROMS; Shchepetkin and McWilliams, 2005) to determine a weighting function for averaging. The method of ROMS is actually designed to compute the state variables at $t = t_{n+2}$ as well as a flow field at $t = t_{n+1}$ which is consistent with surface height at $t = t_{n+2}$ under the discretization of (6.5) by the leap-frog scheme,

$$\frac{\eta^{n+2} - \eta^{n}}{2\Delta t_{\mathrm{cl}}} = -\nabla \cdot \boldsymbol{U}^{n+1} + (P - E + R + I). \tag{6.17}$$

In the framework of the time integration of MRI.COM, only flow field at $t = t_{n+1}$, (U^{n+1}, V^{n+1}), is used among the results of the barotropic submodel. The surface height at baroclinic time levels are computed by (6.17). This is to make the surface height equation be consistent with the continuity equations in a vertical column (Leclair and Madec, 2009). (By setting the runtime parameter `l_global_local_cnsv_ssh = .false.`, an averaged state from the barotropic submodel may be used as η^{n+1} instead of (6.17), although this should be used with care.)

In the old versions of MRI.COM, simple averaging of $(2 \times \Delta t_{\mathrm{cl}}/\Delta t_{\mathrm{tr}} + 1)$ barotropic time steps between the two baroclinic time intervals $[t_n, t_{n+2}]$ is used to obtain state variables at t_{n+1}. From version 4, we use a weighted average as explained by Shchepetkin and McWilliams (2005). Derivation of the weighting function for (U^{n+1}, V^{n+1}), b_m, is briefly summarized below.

First, a weighting shape function to calculate variables at $t = t_{n+2}$ is denoted with $\{a_m\}$ (Note that the target is at $t = t_{n+2}$, not $t = t_{n+1}$). This must satisfy discrete normalization and centroid conditions,

$$\sum_{m=1}^{M^*} a_m \equiv 1, \quad \sum_{m=1}^{M^*} m a_m \equiv 2M, \tag{6.18}$$

where M is the ratio between barotropic-baroclinic time step ($M = \Delta t_{\mathrm{cl}}/\Delta t_{\mathrm{tr}}$), and M^* is the last index at which $a_m > 0$, where $2M \leq M^*$. The weighted averaging is designed so that aliasing between barotropic and baroclinic modes is suppressed as well. With a set of $\{a_m\}$, state variables at the baroclinic time level t_{n+2} is computed as

$$\eta^{n+2} = \sum_{m=1}^{M^*} a_m \eta^m, \quad U^{n+2} = \sum_{m=1}^{M^*} a_m U^m, \quad V^{n+2} = \sum_{m=1}^{M^*} a_m V^m, \tag{6.19}$$

where η^m, U^m, and V^m are instantaneous state variables at the barotropic time level $t = t_m$.

To be consistent with the continuity equation at baroclinic time levels, the vertically integrated continuity equation must satisfy

$$\frac{\eta^{n+2} - \eta^{n}}{2\Delta t_{\mathrm{cl}}} = -\nabla \cdot \mathbf{U}^{n+1}. \tag{6.20}$$

The flow field at the time level $t = t_{n+1}$ can be determined accordingly. Assuming that the vertically integrated continuity equation is advanced in time as

$$\frac{\eta^{m+1} - \eta^{m}}{\Delta t_{\mathrm{tr}}} = -\nabla \cdot \mathbf{U}^{m+\frac{1}{2}}, \tag{6.21}$$

we may obtain the expression for η^m as

$$\eta^m = \eta^0 - \Delta t_{\mathrm{tr}} \sum_{m'=0}^{m-1} \nabla \cdot \mathbf{U}^{m'+\frac{1}{2}}. \tag{6.22}$$

Inserting this into (6.19) and after some manipulations, which is detailed in Shchepetkin and McWilliams (2005), we have

$$\eta^{n+2} = \eta^0 - 2\Delta t_{\mathrm{cl}} \nabla \cdot \sum_{m'=1}^{M^*} b_{m'} \mathbf{U}^{m'-\frac{1}{2}}, \tag{6.23}$$

where $\eta^0 = \eta^n$ and

$$b_{m'} = \frac{1}{2M} \sum_{m=m'}^{M^*} a_m. \tag{6.24}$$

By comparing (6.20) and (6.23), vertically integrated flow field at the baroclinic time level $t = t_{n+1}$ is obtained as

$$U^{n+1} = \sum_{m=1}^{M^*} b_m U^{m-\frac{1}{2}}, \quad V^{n+1} = \sum_{m=1}^{M^*} b_m V^{m-\frac{1}{2}}. \tag{6.25}$$

We require that a set of $\{b_m\}$ satisfies

$$\sum_{m=1}^{M^*} b_m \equiv 1, \quad \sum_{m=1}^{M^*} m b_m \equiv M, \tag{6.26}$$

as well as (6.18).

Specific shape of the weighting function (a_m) for $\tau = m/2M$, $(1 \leq m \leq M^*)$ is given as follows:

$$A(\tau) = A_0 \Big\{ \Big(\frac{\tau}{\tau_0}\Big)^p \Big[1 - \Big(\frac{\tau}{\tau_0}\Big)^q\Big] - r\frac{\tau}{\tau_0} \Big\}, \tag{6.27}$$

where $p = 2$, $q = 2$, $r = 0.2346283$, and A_0 and τ_0 are chosen to satisfy normalization conditions (6.18) and (6.26) iteratively. The initial guess for A_0 and τ_0 is given as follows:

$$A_0 = 1, \quad \tau_0 = \frac{(p+2)(p+q+2)}{(p+1)(p+q+1)}. \tag{6.28}$$

Approximate shape of $\{a_m\}$ and $\{b_m\}$ are shown by red and blue lines of Figure 6.3.

In the following, the discretized momentum equation for the 3-D velocity field under the split-explicit method will be derived. This is to clarify the difference from the one for the 3-D velocity under a normal, fully explicit discretizing method. Let us consider reconstructing the flow field of (6.25) from the momentum equation for the barotropic submodel. In the following, we adopted a simple time stepping scheme (forward scheme) and conceptual notations for representing time levels. Because specific expressions will depend upon the choice of time stepping algorithm, the following equations do not necessarily correspond to the time stepping methods used in the model. But this discrepancy is not essential.

At barotropic time levels, momentum equations are advanced in time as follows:

$$U^{m+1} = U^m + \Delta t_{\mathrm{tr}} f V^{m+\frac{1}{2}} - \Delta t_{\mathrm{tr}} \Big[\frac{(\eta + H)}{\rho_0 h_\mu} \frac{\partial (p_a + \rho_0 g \eta)}{\partial \mu} \Big]^{m+\frac{1}{2}} + \Delta t_{\mathrm{tr}} X, \tag{6.29}$$

$$V^{m+1} = V^m - \Delta t_{\mathrm{tr}} f U^{m+\frac{1}{2}} - \Delta t_{\mathrm{tr}} \Big[\frac{(\eta + H)}{\rho_0 h_\psi} \frac{\partial (p_a + \rho_0 g \eta)}{\partial \psi} \Big]^{m+\frac{1}{2}} + \Delta t_{\mathrm{tr}} Y, \tag{6.30}$$

where $[\cdot]^{m+\frac{1}{2}}$ is an approximate value of $(\cdot)$ at the time level of $m + \frac{1}{2}$, which is dependent on the choice of the time stepping scheme.

Successive summation of (6.29) and (6.30) over $m' = [0, m-1]$ yields

$$U^m = U^0 + \Delta t_{\mathrm{tr}} \sum_{m'=0}^{m-1} f V^{m'+\frac{1}{2}} - \Delta t_{\mathrm{tr}} \sum_{m'=0}^{m-1} \Big[\frac{(\eta + H)}{\rho_0 h_\mu} \frac{\partial (p_a + \rho_0 g \eta)}{\partial \mu} \Big]^{m'+\frac{1}{2}} + m \Delta t_{\mathrm{tr}} X, \tag{6.31}$$

$$V^m = V^0 - \Delta t_{\mathrm{tr}} \sum_{m'=0}^{m-1} f U^{m'+\frac{1}{2}} - \Delta t_{\mathrm{tr}} \sum_{m'=0}^{m-1} \Big[\frac{(\eta + H)}{\rho_0 h_\psi} \frac{\partial (p_a + \rho_0 g \eta)}{\partial \psi} \Big]^{m'+\frac{1}{2}} + m \Delta t_{\mathrm{tr}} Y, \tag{6.32}$$

Applying the time averaging procedure of (6.25) yields

$$\langle U\rangle^{n+1} \equiv \sum_{m=1}^{M^*} b_m U^m \tag{6.33}$$

$$= U^0 + \Delta t_{\mathrm{tr}} \sum_{m=1}^{M^*}\left[b_m \sum_{m'=1}^{m} f V^{m'-\frac{1}{2}}\right] - \Delta t_{\mathrm{tr}} \sum_{m=1}^{M^*}\left\{b_m \sum_{m'=1}^{m}\left[\frac{(\eta+H)}{\rho_0 h_\mu}\frac{\partial(p_a+\rho_0 g\eta)}{\partial\mu}\right]^{m'-\frac{1}{2}}\right\} + \sum_{m=1}^{M^*} m b_m \Delta t_{\mathrm{tr}} X, \tag{6.34}$$

$$\langle V\rangle^{n+1} \equiv \sum_{m=1}^{M^*} b_m V^m \tag{6.35}$$

$$= V^0 - \Delta t_{\mathrm{tr}} \sum_{m=1}^{M^*}\left[b_m \sum_{m'=1}^{m} f U^{m'-\frac{1}{2}}\right] - \Delta t_{\mathrm{tr}} \sum_{m=1}^{M^*}\left\{b_m \sum_{m'=1}^{m}\left[\frac{(\eta+H)}{\rho_0 h_\psi}\frac{\partial(p_a+\rho_0 g\eta)}{\partial\psi}\right]^{m'-\frac{1}{2}}\right\} + \sum_{m=1}^{M^*} m b_m \Delta t_{\mathrm{tr}} Y, \tag{6.36}$$

which are rearranged to have a form

$$\langle U\rangle^{n+1} = U^0 + \Delta t_{\mathrm{cl}} f \langle\langle V\rangle\rangle^{n+\frac{1}{2}} - \Delta t_{\mathrm{cl}}\left\langle\left\langle\frac{(\eta+H)}{\rho_0 h_\mu}\frac{\partial(p_a+\rho_0 g\eta)}{\partial\mu}\right\rangle\right\rangle^{n+\frac{1}{2}} + \Delta t_{\mathrm{cl}} X^n, \tag{6.37}$$

$$\langle V\rangle^{n+1} = V^0 - \Delta t_{\mathrm{cl}} f \langle\langle U\rangle\rangle^{n+\frac{1}{2}} - \Delta t_{\mathrm{cl}}\left\langle\left\langle\frac{(\eta+H)}{\rho_0 h_\psi}\frac{\partial(p_a+\rho_0 g\eta)}{\partial\psi}\right\rangle\right\rangle^{n+\frac{1}{2}} + \Delta t_{\mathrm{cl}} Y^n, \tag{6.38}$$

where $\langle\langle\cdot\rangle\rangle^{n+\frac{1}{2}} \equiv \sum_{m=1}^{M^*} b_m \sum_{m'=1}^{m} (\cdot)^{m'-\frac{1}{2}}$.

On the other hand, the baroclinic momentum equation where surface pressure gradient term is dropped is

$$\frac{u'_{k-\frac{1}{2}}\Delta z^{n+1}_{k-\frac{1}{2}} - u^n_{k-\frac{1}{2}}\Delta z^n_{k-\frac{1}{2}}}{\Delta t_{\mathrm{cl}}} = f[v_{k-\frac{1}{2}}\Delta z_{k-\frac{1}{2}}]^{n+\frac{1}{2}} + F^n_\mu, \tag{6.39}$$

$$\frac{v'_{k-\frac{1}{2}}\Delta z^{n+1}_{k-\frac{1}{2}} - v^n_{k-\frac{1}{2}}\Delta z^n_{k-\frac{1}{2}}}{\Delta t_{\mathrm{cl}}} = -f[u_{k-\frac{1}{2}}\Delta z_{k-\frac{1}{2}}]^{n+\frac{1}{2}} + F^n_\psi. \tag{6.40}$$

This is vertically summed up to give

$$\frac{\sum_{k=1}^N (u'_{k-\frac{1}{2}}\Delta z^{n+1}_{k-\frac{1}{2}}) - \sum_{k=1}^N (u^n_{k-\frac{1}{2}}\Delta z^n_{k-\frac{1}{2}})}{\Delta t_{\mathrm{cl}}} = f\sum_{k=1}^N [v_{k-\frac{1}{2}}\Delta z_{k-\frac{1}{2}}]^{n+\frac{1}{2}} + X^n, \tag{6.41}$$

$$\frac{\sum_{k=1}^N (v'_{k-\frac{1}{2}}\Delta z^{n+1}_{k-\frac{1}{2}}) - \sum_{k=1}^N (v^n_{k-\frac{1}{2}}\Delta z^n_{k-\frac{1}{2}})}{\Delta t_{\mathrm{cl}}} = -f\sum_{k=1}^N [u_{k-\frac{1}{2}}\Delta z_{k-\frac{1}{2}}]^{n+\frac{1}{2}} + Y^n. \tag{6.42}$$

X^n and Y^n are removed from (6.37), (6.38), (6.41), and (6.42) to give

$$\frac{\sum_{k=1}^N (\langle u\rangle^{n+1}\Delta z^{n+1}_{k-\frac{1}{2}}) - \sum_{k=1}^N (u'_{k-\frac{1}{2}}\Delta z^{n+1}_{k-\frac{1}{2}})}{\Delta t_{\mathrm{cl}}} = f\langle\langle V\rangle\rangle^{n+\frac{1}{2}} - f\sum_{k=1}^N [v_{k-\frac{1}{2}}\Delta z_{k-\frac{1}{2}}]^{n+\frac{1}{2}} - \left\langle\left\langle\frac{(\eta+H)}{\rho_0 h_\mu}\frac{\partial(p_a+\rho_0 g\eta)}{\partial\mu}\right\rangle\right\rangle^{n+\frac{1}{2}} \tag{6.43}$$

$$\frac{\sum_{k=1}^N (\langle v\rangle^{n+1}\Delta z^{n+1}_{k-\frac{1}{2}}) - \sum_{k=1}^N (v'_{k-\frac{1}{2}}\Delta z^{n+1}_{k-\frac{1}{2}})}{\Delta t_{\mathrm{cl}}} = -f\langle\langle U\rangle\rangle^{n+\frac{1}{2}} + f\sum_{k=1}^N [u_{k-\frac{1}{2}}\Delta z_{k-\frac{1}{2}}]^{n+\frac{1}{2}} - \left\langle\left\langle\frac{(\eta+H)}{\rho_0 h_\psi}\frac{\partial(p_a+\rho_0 g\eta)}{\partial\psi}\right\rangle\right\rangle^{n+\frac{1}{2}}. \tag{6.44}$$

This is combined with (6.39) and (6.40) to give

$$\frac{\left(u'_{k-\frac{1}{2}} - \overline{u'}^{z} + \langle u \rangle^{n+1}\right)\Delta z^{n+1}_{k-\frac{1}{2}} - u^{n}_{k-\frac{1}{2}}\Delta z^{n}_{k-\frac{1}{2}}}{\Delta t_{\mathrm{cl}}} = f\left[v_{k-\frac{1}{2}}\Delta z_{k-\frac{1}{2}}\right]^{n+\frac{1}{2}} - f\overline{[v]^{n+\frac{1}{2}}}^{z}\Delta z^{n+1}_{k-\frac{1}{2}} + f\langle\langle v\rangle\rangle^{n+\frac{1}{2}}\Delta z^{n+1}_{k-\frac{1}{2}} - \frac{\Delta z^{n+1}_{k-\frac{1}{2}}}{\eta^{n+1}+H}\left\langle\left\langle\frac{(\eta+H)}{\rho_0 h_\mu}\frac{\partial(p_a+\rho_0 g\eta)}{\partial\mu}\right\rangle\right\rangle^{n+\frac{1}{2}} + F^{n}_{\mu} \tag{6.45}$$

$$\frac{\left(v'_{k-\frac{1}{2}} - \overline{v'}^{z} + \langle v \rangle^{n+1}\right)\Delta z^{n+1}_{k-\frac{1}{2}} - v^{n}_{k-\frac{1}{2}}\Delta z^{n}_{k-\frac{1}{2}}}{\Delta t_{\mathrm{cl}}} = -f\left[u_{k-\frac{1}{2}}\Delta z_{k-\frac{1}{2}}\right]^{n+\frac{1}{2}} + f\overline{[u]^{n+\frac{1}{2}}}^{z}\Delta z^{n+1}_{k-\frac{1}{2}} - f\langle\langle u\rangle\rangle^{n+\frac{1}{2}}\Delta z^{n+1}_{k-\frac{1}{2}} - \frac{\Delta z^{n+1}_{k-\frac{1}{2}}}{\eta^{n+1}+H}\left\langle\left\langle\frac{(\eta+H)}{\rho_0 h_\psi}\frac{\partial(p_a+\rho_0 g\eta)}{\partial\psi}\right\rangle\right\rangle^{n+\frac{1}{2}} + F^{n}_{\psi}, \tag{6.46}$$

where $\overline{(\ldots)}^{z}$ denotes the thickness weighted vertical average. This is the momentum balance for the total velocity field under the mode-splitting scheme. In comparison with (6.39) and (6.40), the correction terms appear in the tendency and Coriolis terms owing to the use of the split-explicit method. In the tendency term on the l.h.s., the vertically averaged velocity $(\overline{u'}^{z}, \overline{v'}^{z})$ is replaced by the prediction of the barotropic model $(\langle u\rangle^{n+1}, \langle v\rangle^{n+1})$. Likewise on the r.h.s., the Coriolis term takes a form in which vertical average for $[\mathbf{u}_{k+\frac{1}{2}}]^{n+\frac{1}{2}}$ is replaced by $\langle\langle\mathbf{u}\rangle\rangle^{n+\frac{1}{2}}$.

6.3.2 Update of 3-D state variables at the baroclinic time level

Vertically integrated transport at time $t = t_{n+1}$ is obtained by a weighted averaging of those at barotropic time levels as explained in the previous section. Surface elevation at time $t = t_{n+1}$ is computed by using vertically integrated transport at time t_n, which has been calculated in the previous time step and stored, and updated with the leap frog scheme:

$$\frac{\eta^{n+1} - \eta^{n-1}}{2\Delta t} + \nabla\cdot\boldsymbol{U}^{n} = P - E + R + I, \tag{6.47}$$

as explained in Section 6.3.1.

With this surface elevation, the height of the vertical column and the volume of the grid cells in the column may be determined (see Chapter 3). Once the volume is determined, 3D state variables at time $t = t_{n+1}$ may be computed. The velocity field may be computed as follows:

- A provisional baroclinic velocity field (u'^{n+1}, v'^{n+1}) is computed using the tendency terms computed by the baroclinic module.
- The provisional velocity (u'^{n+1}, v'^{n+1}) is integrated over the whole column and the vertical mean of the provisional velocity is computed.
- The vertical mean velocity is subtracted from the provisional velocity first and the actual mean velocity based on (U^{n+1}, V^{n+1}) is added instead in order to yield the final velocity field (u^{n+1}, v^{n+1}).

These operations correspond to the expression for the velocity at the $(n+1)$th time step in the tendency term of (6.45), (6.46), for example, $u'_{k-1/2} - \overline{u'}^{z} + \langle u\rangle^{n+1}$.

Because (6.47) is consistent with the continuity equation for the T-cell, computation of tendency of tracer due to advection is both conservative and constancy preserving. This method guarantees that tracer is conserved both globally and locally.

Note that body forcing for the uppermost layer such as wind-forcing and restoration of temperature and salinity to the prescribed values may act differently for grid cells with different width. The body force for the uppermost layer becomes

$$\left(\frac{\partial u}{\partial t}, \frac{\partial v}{\partial t}\right)\Big|_{k=\frac{1}{2}} = \ldots + \frac{1}{\rho_0}\frac{(\tau_\mu, \tau_\psi)}{\Delta z_{\frac{1}{2}}}, \tag{6.48}$$

where (τ_μ, τ_ψ) are the wind stress at the surface (momentum flux), and $\Delta z_{\frac{1}{2}}$ is the variable thickness of the uppermost layer. Thus, the uppermost layer is more accelerated when this layer is thinner than the standard value.

When the restoring condition is applied at the surface, the corresponding temperature and salinity fluxes are

$$F_z^\theta = -\frac{1}{\gamma_\theta}(\theta - \theta^*)\Delta z_{\frac{1}{2}}, \qquad \left.\frac{\partial \theta}{\partial t}\right|_{k=\frac{1}{2}} = \ldots + \frac{F_z^\theta}{\Delta z_{\frac{1}{2}}}, \tag{6.49}$$

$$F_z^S = -\frac{1}{\gamma_s}(S - S^*)\Delta z_{\frac{1}{2}}, \qquad \left.\frac{\partial S}{\partial t}\right|_{k=\frac{1}{2}} = \ldots + \frac{F_z^S}{\Delta z_{\frac{1}{2}}}. \tag{6.50}$$

Thus, the temperature and salinity are more strongly restored to the prescribed values when this layer is thinner than the standard value.

6.4 Horizontal diffusivity of sea surface height

The null mode, or checkerboard pattern, would appear in the sea surface height field commonly in the Arakawa B-grid models. For the purpose of suppressing this mode, a weak horizontal diffusion of sea surface height may be included in the vertically integrated continuity equation,

$$\frac{\partial \eta}{\partial t} + \frac{1}{h_\mu h_\psi}\left\{\frac{\partial (h_\psi U)}{\partial \mu} + \frac{\partial (h_\mu V)}{\partial \psi}\right\} = \mathcal{D}(\eta) + (P - E + R + I) \tag{6.51}$$

where $\mathcal{D}$ is the diffusion operator (Chapter 12.9 in Griffies (2004)). The diffusion operator mixes a sea surface height in each direction of the model coordinates with the harmonic scheme. The specific form of the harmonic-type diffusivity is represented as follows:

$$\mathcal{D}(\eta) = \frac{1}{h_\mu h_\psi}\left\{\frac{\partial}{\partial \mu}\left(\frac{h_\psi \kappa_H}{h_\mu}\frac{\partial \eta}{\partial \mu}\right) + \frac{\partial}{\partial \psi}\left(\frac{h_\mu \kappa_H}{h_\psi}\frac{\partial \eta}{\partial \psi}\right)\right\} \tag{6.52}$$

$$= \frac{1}{h_\mu h_\psi}\left\{\frac{\partial h_\psi F_\mu^\eta}{\partial \mu} + \frac{\partial h_\mu F_\psi^\eta}{\partial \psi}\right\} \tag{6.53}$$

where κ_H is the horizontal diffusion coefficients and the diffusive fluxes are represented by

$$\mathbf{F}^\eta = -\Big(\frac{\kappa_H}{h_\mu}\frac{\partial \eta}{\partial \mu}, \frac{\kappa_H}{h_\psi}\frac{\partial \eta}{\partial \psi}\Big). \tag{6.54}$$

Therefore, continuity equation may be rewritten as follows:

$$\frac{\partial \eta}{\partial t} + \frac{1}{h_\mu h_\psi}\left\{\frac{\partial [h_\psi (U + F_\mu^\eta)]}{\partial \mu} + \frac{\partial [h_\mu (V + F_\psi^\eta)]}{\partial \psi}\right\} = (P - E + R + I). \tag{6.55}$$

If the horizontal diffusivity is non-zero for sea surface height, $U^* = U + F_\mu^\eta$ and $V^* = V + F_\psi^\eta$ are treated as the vertically integrated transport velocity, which are divided by the column height to replace the vertical mean velocity based on (U, V) which have been contained in the 3-D velocity field used to advect momentum and tracers. It should be noted that additional restart files are necessary when horizontal diffusion is applied to SSH. This is because $(F_\mu^\eta, F_\psi^\eta)$ are needed to obtain sea surface height for the new time step. MRI.COM provides namelist `nmlrs_ssh_dflx_x` and `nmlrs_ssh_dflx_y` for this purpose.

6.5 Inclusion of tidal effect

This section explains the tide option (`TIDE`) in MRI.COM.

6.5.1 Tide producing term in the momentum equation

Tidal forcing can be introduced into the barotropic part of the momentum equations (6.1) and (6.2) as follows (e.g., Schiller, 2004):

$$\frac{\partial U}{\partial t} - fV = -\frac{(\eta + H)}{\rho_0 h_\mu}\frac{\partial (p_a + \rho_0 g \eta)}{\partial \mu} - \frac{g(\eta + H)}{h_\mu}\frac{\partial}{\partial \mu}[(1 - \alpha)\eta - \beta \eta_{\mathrm{eq}}] + X, \tag{6.56}$$

$$\frac{\partial V}{\partial t} + fU = -\frac{(\eta + H)}{\rho_0 h_\psi}\frac{\partial (p_a + \rho_0 g \eta)}{\partial \psi} - \frac{g(\eta + H)}{h_\psi}\frac{\partial}{\partial \psi}[(1 - \alpha)\eta - \beta \eta_{\mathrm{eq}}] + Y, \tag{6.57}$$

Table6.1 Constants of major tidal modes

n	Tidal Mode	K, m	σ, 10^{-4} /sec	χ, deg
1	K_1, declination luni-solar	0.141565	0.72921	$h_0 + 90$
2	Q_1, principal lunar	0.100514	0.67598	$h_0 - 2s_0 + 90$
3	P_1, principal solar	0.046843	0.72523	$-h_0 - 90$
4	Q_1, elliptical lunar	0.019256	0.64959	$h_0 - 3s_0 + p_0 - 90$
5	M_2, principal lunar	0.242334	1.40519	$2h_0 - 2s_0$
6	S_2, principal solar	0.112841	1.45444	0
7	N_2, elliptical lunar	0.046398	1.37880	$2h_0 - 3s_0 + p_0$
8	K_2, declination luni-solar	0.030704	1.45842	$2h_0$

Here h_0, s_0, and p_0 are the mean longitudes of the sun and moon and the lunar perigee at Greenwich midnight: $h_0 = 279.69668 + 36000.768930485T + 3.03 \times 10^4 T^2$, $s_0 = 270.434358 + 481267.88314137T - 0.001133T^2 + 1.9 \times 10^{-6} T^3$, $p_0 = 334.329653 + 4069.0340329575T - 0.010325T^2 - 1.2 \times 10^{-5} T^3$, where $T = (27392.500528 + 1.0000000356D)/36525$, $D = d + 365(y - 1975) + \mathrm{Int}[(y - 1973)/4]$, d is the day numbe of the year ($d = 1$ for January 1), $y \geq 1975$ is the year number, and Int$[x]$ is the integral part of x.

where α defines self-attraction and loading of the ocean tides, $\beta = 1 + k - h$ defines effect of tide-generating potential and correction due to earth tides with k and h being Love numbers, and η_{eq} is equilibrium tide, or astronomical tide-generating potential. In MRI.COM, we usually set $\alpha = 0.88$ and $\beta = 0.7$.

The eight primary constituents that consist of the four largest equilibrium tides of the diurnal and semi-diurnal species (K_1, O_1. $P_1, Q_1, M_2, S_2, N_2, K_2$) may be included in the tide producing potential η_{eq} of MRI.COM. Following Schwiderski (1980), we write the n-th ($n = [1, 4]$) diurnal equilibrium tide as

$$\begin{aligned}\eta_{\mathrm{eq},n} &= K_n \cos^2\phi \cos(\sigma_n t + \chi_n + 2\lambda) \\ &= K_n \cos^2\phi [\cos(\sigma_n t + \chi_n)\cos 2\lambda - \sin(\sigma_n t + \chi_n)\sin 2\lambda],\end{aligned} \tag{6.58}$$

and the n-th semi-diurnal component ($n = [5, 8]$) as

$$\begin{aligned}\eta_{\mathrm{eq},n} &= K_n \sin 2\phi \cos(\sigma_n t + \chi_n + \lambda) \\ &= K_n \sin 2\phi [\cos(\sigma_n t + \chi_n)\cos\lambda - \sin(\sigma_n t + \chi_n)\sin\lambda].\end{aligned} \tag{6.59}$$

The meaning of the mathematical symbols is as follows:

t	universal standard time in seconds
λ	east longitude
ϕ	latitude
K	amplitude of partial equilibrium tide in meters
σ	frequency of partial equilibrium tide in sec^{-1}
χ	astronomical argument of partial equilibrium tide relative to Greenwich midnight

And constants are listed on Table 6.1.

6.5.2 Separation of linear responses to tidal forcing

By including tidal forcing, the balance in the basic fields solved without tides will be modified through non-linear terms of the equations. In addition to the non-linear terms, self-attraction and loading terms in (6.56) and (6.57) will modify the relationships between the sea surface height gradient and the barotropic currents. That is, the solution without astronomical tide-generating potential ($\eta_{\mathrm{eq}} = 0$) will be different than that solved with standard equations without self-attraction and loading terms.

To resolve the possible problem that the terms specialized for tides affect the basic fields unintentionally, our tide scheme calculates the tidal fields separately from the basic fields within the barotropic submodel as explained by Sakamoto et al. (2013). The essence of the solution method is explained below. First, we rewrite the basic equation of the barotropic submodel in the following form that highlights the terms that may be specialized for tides:

$$\frac{\partial \mathbf{U}}{\partial t} + f\mathbf{k} \times \mathbf{U} = -g(\eta + H)\nabla(\eta - \beta\eta_{\mathrm{eq}} - \eta_{\mathrm{SAL}}) + \mathbf{F}^{\mathrm{horz}} + \frac{\tau^{\mathrm{btm}}}{\rho_0} + \mathbf{X}', \tag{6.60}$$

where $\mathbf{F}^{\mathrm{horz}}$ is the vertically integrated horizontal viscosity parameterization terms and τ^{btm} is the bottom friction terms that may be specialized for tidal currents. They are separated from $\mathbf{X}$ defined by (6.3) and (6.4) and $\mathbf{X}' \equiv \mathbf{X} - \mathbf{F}^{\mathrm{horz}} - \tau^{\mathrm{btm}}/\rho_0$.

Note also that atmospheric pressure term is dropped for brevity. Continuity equation is

$$\frac{\partial \eta}{\partial t} + \nabla \cdot \mathbf{U} = F_w, \tag{6.61}$$

where $F_w \equiv P - E + R + I$ is surface fresh water forcing that will be enter the system through the basic fields.

Next, the variables are decomposed into the linear tidal component and the basic component,

$$\mathbf{U} = \mathbf{U}_b + \mathbf{U}_{lt} \tag{6.62}$$

$$\eta = \eta_b + \eta_{lt} \tag{6.63}$$

$$\mathbf{F}^{\mathrm{horz}} = \mathbf{F}_b^{\mathrm{horz}} + \mathbf{F}_{lt}^{\mathrm{horz}} \tag{6.64}$$

$$\tau^{\mathrm{btm}} = \tau_b^{\mathrm{btm}} + \tau_{lt}^{\mathrm{btm}}, \tag{6.65}$$

where "lt" refers to linear tidal component and "b" refers to basic fields. Now we decompose (6.60) and (6.61) to obtain governing equations for each of the two components.

For linear tidal component:

$$\frac{\partial \mathbf{U}_{lt}}{\partial t} + f\mathbf{k} \times \mathbf{U}_{lt} = -g(\eta + H)\nabla(\eta_{lt} - \beta\eta_{\mathrm{eq}} - \eta_{\mathrm{SAL}}) + \mathbf{F}_{lt}^{\mathrm{horz}} + \frac{\tau_{lt}^{\mathrm{btm}}}{\rho_0}, \tag{6.66}$$

$$\frac{\partial \eta_{lt}}{\partial t} + \nabla \cdot \mathbf{U}_{lt} = 0, \tag{6.67}$$

where we assume that self-attraction and loading acts only to linear tidal component in such a way as $\eta_{\mathrm{SAL}} = (1 - \alpha)\eta_{lt}$.

For the basic component:

$$\frac{\partial \mathbf{U}_b}{\partial t} + f\mathbf{k} \times \mathbf{U}_b = -g(\eta + H)\nabla\eta_b + \mathbf{F}_b^{\mathrm{horz}} + \frac{\tau_b^{\mathrm{btm}}}{\rho_0} + \mathbf{X}', \tag{6.68}$$

$$\frac{\partial \eta_b}{\partial t} + \nabla \cdot \mathbf{U}_b = F_w. \tag{6.69}$$

In the above decomposition, the linear tidal component represents only the linear response to tidal forcing, and the secondary effects of tide, such as tidal advection and internal tides, are represented by the basic component. The linear terms in the barotropic equations, such as the Coriolis force and the Laplacian horizontal viscosity with a constant viscosity coefficient may be split into the basic and linear tidal components naturally. The bottom friction term (τ^{btm}) is non-linear and should be treated carefully. The bottom friction term (see Section 7.3.6 for details) is expressed as

$$\tau^{\mathrm{btm}} = -\rho_0 C_D |\mathbf{u}| \mathbf{T}_\theta \mathbf{u}, \tag{6.70}$$

where C_D is a drag coefficient and $\mathbf{T}_\theta$ is a matrix representing horizontal veering with an angle of θ,

$$\mathbf{T}_\theta = \begin{pmatrix} \cos\theta & -\sin\theta \\ \sin\theta & \cos\theta \end{pmatrix}. \tag{6.71}$$

Sum of the two components are used for the scalar part ($|\mathbf{u}|$) and only the vector part is decomposed:

$$\tau_b^{\mathrm{btm}} = -\rho_0 C_D |\mathbf{u}_b + \mathbf{u}_{lt}| \mathbf{T}_\theta \mathbf{u}_b, \tag{6.72}$$

$$\tau_{lt}^{\mathrm{btm}} = -\rho_0 C_D |\mathbf{u}_b + \mathbf{u}_{lt}| \mathbf{T}_\theta \mathbf{u}_{lt}. \tag{6.73}$$

Similarly, when the horizontal viscosity parameterization is non-linear as in the Smagorinsky scheme, the coefficient part (e.g., ν_H in the equations below) is calculated by using the full velocity and the decomposed fields are applied to the viscosity operator. When the horizontal tension D_T and shear D_S of the velocity field,

$$D_T = h_\psi \frac{\partial}{h_\mu \partial \mu}\Big(\frac{u}{h_\psi}\Big) - h_\mu \frac{\partial}{h_\psi \partial \psi}\Big(\frac{v}{h_\mu}\Big), \tag{6.74}$$

$$D_S = h_\mu \frac{\partial}{h_\psi \partial \psi}\Big(\frac{u}{h_\mu}\Big) + h_\psi \frac{\partial}{h_\mu \partial \mu}\Big(\frac{v}{h_\psi}\Big), \tag{6.75}$$

is used to calculate horizontal viscosity as

$$F_u^{\mathrm{horz}} = \frac{1}{h_\psi^2}\frac{\partial}{h_\mu \partial \mu}\left(h_\psi^2 \nu_H D_T\right) + \frac{1}{h_\mu^2}\frac{\partial}{h_\psi \partial \psi}\left(h_\mu^2 \nu_H D_S\right), \tag{6.76}$$

$$F_v^{\mathrm{horz}} = \frac{1}{h_\psi^2}\frac{\partial}{h_\mu \partial \mu}\left(h_\psi^2 \nu_H D_S\right) - \frac{1}{h_\mu^2}\frac{\partial}{h_\psi \partial \psi}\left(h_\mu^2 \nu_H D_T\right), \tag{6.77}$$

where ν_H is the horizontal viscosity coefficient, $\mathbf{u}_b$ and $\mathbf{u}_{lt}$ is used for D_T and D_S to calculate $\mathbf{F}_b^{\mathrm{horz}}$ and $\mathbf{F}_{lt}^{\mathrm{horz}}$ by using (6.76) and (6.77).

By formulation, $\mathbf{F}^{\mathrm{horz}}$, τ^{btm}, and $\mathbf{X}'$ are computed at the baroclinic time level of n and kept fixed during the integration of barotropic submodel. However, when the barotropic field varies significantly during the integration, which is expected when tidal forcing is included, $\mathbf{F}^{\mathrm{horz}}$ and τ^{btm} should be allowed to vary with the evolution of barotropic velocity field. In this case, $\mathbf{F}_{lt}^{\mathrm{horz}}$ and τ_{lt}^{btm} in (6.66) may be replaced by the viscosity parameterization suitable to the tidal velocity fields (represented by $\mathbf{F}_{tide}^{\mathrm{horz}}$ and $\tau_{tide}^{\mathrm{btm}}$, respectively). Then, (6.66) and (6.68) becomes,

$$\frac{\partial \mathbf{U}_{lt}}{\partial t} + f\mathbf{k}\times\mathbf{U}_{lt} = -g(\eta+H)\nabla(\alpha\eta_{lt} - \beta\eta_{\mathrm{eq}}) + \mathbf{F}_{tide}^{\mathrm{horz}} + \frac{\tau_{tide}^{\mathrm{btm}}}{\rho_0}, \tag{6.78}$$

$$\frac{\partial \mathbf{U}_{b}}{\partial t} + f\mathbf{k}\times\mathbf{U}_{b} = -g(\eta+H)\nabla\eta_b + \mathbf{X} - \mathbf{F}_{lt}^{\mathrm{horz}} - \frac{\tau_{lt}^{\mathrm{btm}}}{\rho_0}. \tag{6.79}$$

A sequence of operations explained in Section 6.3.1 is applied to both basic and tidal components. But now we use surface height at time level $t = t_n$ as the height of column applied to the pressure gradient term during the barotropic subcycle. The weighted average of the barotropic fields is written as follows:

$$\begin{aligned}\langle \mathbf{U}_{lt}\rangle^{n+1} &= \mathbf{U}_{lt}^0 - \Delta t_{\mathrm{cl}} f\mathbf{k}\times\langle\langle \mathbf{U}_{lt}\rangle\rangle^{n+\frac{1}{2}} - \Delta t_{\mathrm{cl}} g(\eta^n + H)\Big\langle\Big\langle \nabla(\alpha\eta_{lt} - \beta\eta_{\mathrm{eq}})\Big\rangle\Big\rangle^{n+\frac{1}{2}} \\ &\quad + \Delta t_{\mathrm{cl}}\langle\langle \mathbf{F}_{tide}^{\mathrm{horz}}\rangle\rangle^{n+\frac{1}{2}} + \frac{1}{\rho_0}\Delta t_{\mathrm{cl}}\langle\langle \tau_{tide}^{\mathrm{btm}}\rangle\rangle^{n+\frac{1}{2}},\end{aligned} \tag{6.80}$$

$$\langle \mathbf{U}_{b}\rangle^{n+1} = \mathbf{U}_{b}^0 - \Delta t_{\mathrm{cl}} f\mathbf{k}\times\langle\langle \mathbf{U}_{b}\rangle\rangle^{n+\frac{1}{2}} - \Delta t_{\mathrm{cl}} g(\eta^n + H)\Big\langle\Big\langle \nabla\eta_b\Big\rangle\Big\rangle^{n+\frac{1}{2}} + \Delta t_{\mathrm{cl}}\Big(\mathbf{X} - \mathbf{F}_{lt}^{\mathrm{horz}} - \frac{\tau_{lt}^{\mathrm{btm}}}{\rho_0}\Big)^n. \tag{6.81}$$

These are summed and then combined with the baroclinic part (6.39) and (6.40) to give

$$\begin{aligned}\frac{(\langle\mathbf{u}\rangle^{n+1} + \mathbf{u}'_{k-\frac{1}{2}} - \overline{\mathbf{u}'}^z)\Delta z_{k-\frac{1}{2}}^{n+1} - \mathbf{u}_{k-\frac{1}{2}}^n\Delta z_{k-\frac{1}{2}}^n}{\Delta t_{\mathrm{cl}}} &= - f\mathbf{k}\times\langle\langle\mathbf{u}\rangle\rangle^{n+\frac{1}{2}}\Delta z_{k-\frac{1}{2}}^{n+1} - f\mathbf{k}\times[\mathbf{u}_{k-\frac{1}{2}}\Delta z_{k-\frac{1}{2}}]^{n+\frac{1}{2}} + f\mathbf{k}\times\overline{[\mathbf{u}]^{n+\frac{1}{2}}}^z\Delta z_{k-\frac{1}{2}}^{n+1} \\ &\quad - g\Delta z_{k-\frac{1}{2}}^{n+1}\frac{\eta^n + H}{\eta^{n+1}+H}\Big\langle\Big\langle\nabla(\eta_b + \alpha\eta_{lt} - \beta\eta_{\mathrm{eq}})\Big\rangle\Big\rangle^{n+\frac{1}{2}} \\ &\quad + \Delta z_{k-\frac{1}{2}}^{n+1}\frac{\langle\langle\mathbf{F}_{tide}^{\mathrm{horz}}\rangle\rangle^{n+\frac{1}{2}} - (\mathbf{F}_{lt}^{\mathrm{horz}})^n}{\eta^{n+1}+H} + \Delta z_{k-\frac{1}{2}}^{n+1}\frac{\langle\langle\tau_{tide}^{\mathrm{btm}}\rangle\rangle^{n+\frac{1}{2}} - (\tau_{lt}^{\mathrm{btm}})^n}{\rho_0(\eta^{n+1}+H)} + \Delta z_{k-\frac{1}{2}}^{n+1}\mathbf{F}^n.\end{aligned} \tag{6.82}$$

There is no strong restriction on the form of the viscosity parameterization applied to the tidal velocity fields. However, by using a common form for both baroclinic and barotropic fields, depth integrated viscosity terms in (6.82) would cancel when barotropic and baroclinic mode are synchronous. In MRI.COM, the bottom friction for the linear tidal component is calculated as follows:

$$\tau_{tide}^{\mathrm{btm}} = -\rho_0 C_D\left|\frac{\mathbf{U}_b + \mathbf{U}_{lt}}{\eta + H}\right|\mathbf{T}_\theta\frac{\mathbf{U}_{lt}}{\eta + H}. \tag{6.83}$$

Horizontal viscosity parameterization is the Laplacian operator with the viscosity coefficient fixed in time.

The solution method to predict the two components of the barotropic mode is schematically illustrated by Figure 6.4. On starting the barotropic submodel, the total barotropic mode is split into the basic and the linear tidal components (U_b, η_b, U_{lt}, and η_{lt}) and the time evolution is calculated separately. A simple sum of the two modes is returned to the main part of OGCM. For the next step, the total and the linear tidal components are retained. The basic component is calculated by subtracting the tidal part from the total.

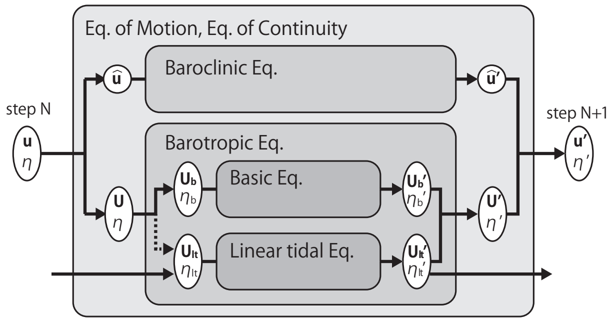

Figure6.4 Schematic figure of the separating basic and linear tidal component of the barotropic mode

6.5.3 Nesting experiment with tide

The tide scheme can work together with the nesting schemes in MRI.COM. This subsection describes briefly how the tide scheme works with on-line nesting and off-line one-way nesting methods. See Chapter 18 for the general explanation of the nesting schemes.

For on-line nesting, the tide models communicate each other between the parent low-resolution model and the child high-resolution model in order to predict tides at the next step in the same manner as the barotropic model. The lateral boundaries of the child model receive $\mathbf{U}_{lt}$ and η_{lt} from the parent model every steps of the barotropic mode in the both cases of one-way and two-way nesting. On the other hand, in the case of two-way nesting with the "replace" configuration, the internal region of the parent model receives them from the child model.

For off-line one-way nesting, the communication process of the tide model is also the same as that of the barotropic model. The parent model saves $\mathbf{U}_{lt}$ and η_{lt} on bands corresponding to the lateral boundaries of the child model. The child model reads the files and interpolates them spatially and temporally to the lateral boundaries every barotropic steps. It should be noted that other lateral boundary data output by the parent model, such as three-dimensional velocity, sea surface height and x and y transports, also includes the linear tidal component. That is, the parent model saves $\mathbf{u}$, $\mathbf{U}_b + \mathbf{U}_{lt}$ and $\eta_b + \eta_{lt}$.

As a special function for off-line one-way nesting, the child model can be executed under tidal forcing even when the parent model does not include tides. That is, users can run the parent model without `TIDE`, while the child model with it. In this case, in advance, users have to create files for the child model boundaries of $\mathbf{U}_{lt}$ and η_{lt} in the same format as the parent model output. The MXE (see Section 21.6) package offers a tool for it based on the Matsumoto et al. (2000)'s dataset in the directory `prep/nest/offline/`. In addition, boundary files output by the parent model do not include the tidal component, which is different from the case that the parent model includes tides. Users have to specify namelist to handle this difference (`l_parent_include_tide = .false.` in `nml_submodel_tide`).

6.6 Usage

Behavior of the barotropic model at run time is specified by the three namelist blocks shown on Tables 6.2 through 6.4. For the initial condition of the model, restart files must be prepared for five variables: sea surface height, X- and Y-ward barotropic transports, and X- and Y-ward transports due to SSH diffusion (unnecessary if `l_global_local_cnsv_ssh = .false.`).

In addition, following model options are available.

`TIDE`: Tide producing forcing is activated
Specify parameters of the tide model by namelist `nml_tide_model`, the initial condition by `nml_tide_run`, and forced tidal constituents by `nml_tide_forcing`. If a specific state is used for the initial condition, three restart files must be prepared. See Section 6.5 for details.

`SLP`: Sea surface is elevated/depressed according to surface atmospheric pressure
Give atmospheric sea-level pressure, p_a in (6.1) and (6.2), to the model by namelist `nml_force_data` (See Table 14.4).

`FSVISC`: Explicit viscosity is added to the barotropic momentum equation
Specify the horizontal viscosity coefficient by namelist `nml_barotropic_visc_horz`. See Section 6.2 for the time discretization method.

See docs/README.Namelist for namelist details.

Table6.2 Namelist nml_barotropic_model for the specifying basic features of the barotropic model (see Section 6.6)

variable	units	description	usage
dt_barotropic_sec	sec	time step interval	required
l_global_local_cnsv_ssh	logical	how to predict sea surface height (Section 6.3.1)	default = .true.

Table6.3 Namelist nml_barotropic_run for starting the barotropic model (see Section 6.6)

variable	units	description	usage
l_rst_barotropic_in	logical	read initial restart for sea surface and transport or not	default = l_rst_in
l_rst_barotropic_dflx_in	logical	read initial restart for diffusive flux of SSH or not (Section 6.4)	default = l_rst_barotropic_in, valid only when l_global_local_cnsv_ssh = .true.

Table6.4 Namelist nml_barotropic_diff for specifying SSH diffusion (see Section 6.6)

variable	units	description	usage
ssh_diff_cm2ps	$cm^2\ s^{-1}$	diffusivity for SSH (Section 6.4)	default = zero

Chapter 7

Equations of motion (baroclinic component)

This chapter explains the advection terms (Section 7.1), the pressure gradient terms (Section 7.2), and the viscosity terms (Section 7.3) of the hydrostatic momentum equation. The basic equations (2.33) and (2.34) in Chapter 2 are re-written:

$$
\begin{aligned}
&\frac{\partial(z_s u)}{\partial t}+\frac{1}{h_\mu h_\psi}\left\{\frac{\partial(z_s h_\psi uu)}{\partial\mu}+\frac{\partial(z_s h_\mu vu)}{\partial\psi}\right\}+\frac{\partial(z_s\dot{s}u)}{\partial s}+z_s\frac{v}{h_\mu h_\psi}\left(\frac{\partial h_\mu}{\partial\psi}u-\frac{\partial h_\psi}{\partial\mu}v\right)-z_s f v\\
&\quad=-z_s\frac{1}{\rho_0 h_\mu}\frac{\partial(p_a+g\rho_0\eta)}{\partial\mu}-z_s\frac{1}{\rho_0 h_\mu}\frac{\partial}{\partial\mu}\Big(g\int_{z(z^*)}^{\eta}\rho' dz\Big)-z_s\frac{g\rho'}{\rho_0 h_\mu}\frac{\partial z}{\partial\mu}\\
&\quad\quad+z_s\frac{1}{\rho_0}(\nabla\cdot\tau_{\text{horizontal strain}})_u+z_s\frac{1}{z_s}\frac{\partial}{\partial s}\Big(\frac{\nu_V}{z_s}\frac{\partial u}{\partial s}\Big),
\end{aligned}
\tag{7.1}
$$

$$
\begin{aligned}
&\frac{\partial(z_s v)}{\partial t}+\frac{1}{h_\mu h_\psi}\left\{\frac{\partial(z_s h_\psi uv)}{\partial\mu}+\frac{\partial(z_s h_\mu vv)}{\partial\psi}\right\}+\frac{\partial(z_s\dot{s}v)}{\partial s}+z_s\frac{u}{h_\mu h_\psi}\left(\frac{\partial h_\psi}{\partial\mu}v-\frac{\partial h_\mu}{\partial\psi}u\right)+z_s f u\\
&\quad=-z_s\frac{1}{\rho_0 h_\psi}\frac{\partial(p_a+g\rho_0\eta)}{\partial\psi}-z_s\frac{1}{\rho_0 h_\psi}\frac{\partial}{\partial\psi}\Big(g\int_{z(z^*)}^{\eta}\rho' dz\Big)-z_s\frac{g\rho'}{\rho_0 h_\psi}\frac{\partial z}{\partial\psi}\\
&\quad\quad+z_s\frac{1}{\rho_0}(\nabla\cdot\tau_{\text{horizontal strain}})_v,+z_s\frac{1}{z_s}\frac{\partial}{\partial s}\Big(\frac{\nu_V}{z_s}\frac{\partial v}{\partial s}\Big).
\end{aligned}
\tag{7.2}
$$

One of the unique characteristics of MRI.COM's momentum advection terms is that there are oblique exchanges of momentum between U-cells that share only a corner. This scheme enables the flow field around and over the bottom topography to be naturally expressed. Furthermore, quasi-enstrophies, $(\partial u/\partial y)^2$ and $(\partial v/\partial x)^2$, for the U-cells away from land are conserved in calculating the momentum advection for horizontally non-divergent flows. The description of momentum advection in Section 7.1 is based on Ishizaki and Motoi (1999).

The discrete expressions for the viscosity terms in the momentum equations are based on generalized orthogonal coordinates. A harmonic operator is used as the default assuming a no-slip condition on the land-sea boundaries. A biharmonic operator (`VISBIHARM` option) and a parameterization of viscosity as a function of deformation rate (`SMAGOR` option) may also be used.

7.1 Advection terms

Chapter 5 demonstrated that the mass fluxes used for calculating momentum advection are identical to those for the mass continuity of the U-cell, and that they are obtained by an averaging operation (5.21) of those for the T-cell mass continuity (5.12) to (5.18). This is the preliminaries for constructing the general mass flux form over an arbitrary bottom and coastal topography. Its vertical part can express diagonally upward mass fluxes over bottom relief and its horizontal part can express horizontally diagonal mass fluxes along coast lines (Ishizaki and Motoi, 1999).

Here we explain how to obtain the mass fluxes used in the momentum advection and how to get the finite difference expression of the advection terms.

The horizontal subscript indices of variables are integers for the T-point (i, j), and therefore, $(i+\frac{1}{2}, j+\frac{1}{2})$ for the U-point. In the vertical direction, integer k is used for the level of the vertical mass fluxes and the level for the T- and U-points a half vertical grid size lower is expressed by $k+\frac{1}{2}$ (Figure 3.3(a)).

7.1.1 Vertical mass fluxes and its momentum advection

According to the definition (5.12) and (5.21) in Chapter 5, the vertical mass flux at the upper surface, level k, of the U-cell $(i+\frac{1}{2}, j+\frac{1}{2}, k+\frac{1}{2})$, $\overline{W}^U_{i+\frac{1}{2},j+\frac{1}{2},k}$, is defined by surrounding W^T as

$$\overline{W}^U_{i+\frac{1}{2},j+\frac{1}{2},k} = \frac{W^T_{i,j,k}}{N_{i,j,k+\frac{1}{2}}} + \frac{W^T_{i+1,j,k}}{N_{i+1,j,k+\frac{1}{2}}} + \frac{W^T_{i,j+1,k}}{N_{i,j+1,k+\frac{1}{2}}} + \frac{W^T_{i+1,j+1,k}}{N_{i+1,j+1,k+\frac{1}{2}}}, \tag{7.3}$$

where $N_{i,j,k+\frac{1}{2}}$ is the number of sea grid cells around the T-point $T_{i,j}$ in layer $k+\frac{1}{2}$.

On the other hand, the vertical mass flux at the bottom surface, level k, of the U-cell $(i+\frac{1}{2}, j+\frac{1}{2}, k-\frac{1}{2})$, $\mathcal{W}^U_{i+\frac{1}{2},j+\frac{1}{2},k}$ is defined as

$$\mathcal{W}^U_{i+\frac{1}{2},j+\frac{1}{2},k} = \frac{W^T_{i,j,k}}{N_{i,j,k-\frac{1}{2}}} + \frac{W^T_{i+1,j,k}}{N_{i+1,j,k-\frac{1}{2}}} + \frac{W^T_{i,j+1,k}}{N_{i,j+1,k-\frac{1}{2}}} + \frac{W^T_{i+1,j+1,k}}{N_{i+1,j+1,k-\frac{1}{2}}}. \tag{7.4}$$

Though W^T are continuous at the boundary of vertically adjacent T-cells, $\overline{W}^U_{i+\frac{1}{2},j+\frac{1}{2},k}$ and $\mathcal{W}^U_{i+\frac{1}{2},j+\frac{1}{2},k}$ seem to be discontinuous at the boundary when N are vertically different, for example, $N_{i,j,k+\frac{1}{2}} < N_{i,j,k-\frac{1}{2}}$, over the bottom relief. However, this apparent discrepancy can be consistently interpreted by introducing diagonally upward or downward mass fluxes as shown below.

a. One-dimensional variation of bottom relief

We first consider a case in which the bottom depth varies in one direction like a staircase and a barotropic current flows from the left to the right over the topography. Figure 7.1(a) indicates the mass continuity for T-cells to conserve barotropy in shallow regions (the U-points are just intermediate between T-points) . Figure 7.1(b) depicts the mass continuity for U-cells, derived from those for adjacent T-cells. Except for fluxes just on the bottom slope, each flux is obtained as a mean value of neighboring fluxes for T-cells. Just on the bottom slope, we must introduce a flux that flows along the slope to ensure mass continuity. The lowermost U-cells at the slope have nonzero vertical flux at the bottom. The barotropy of the flow and the distribution of vertical velocity are thereby kept reasonable for U-cell fluxes.

(a)

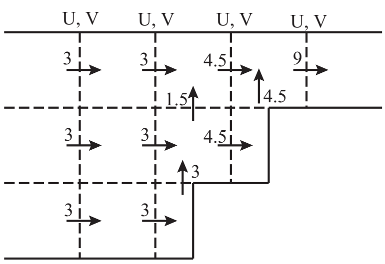

(b)

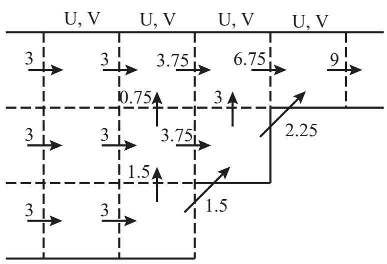

Figure7.1 (a) Two-dimensional mass fluxes for T-cells on a stair-like topography. (b) Two-dimensional mass fluxes for U-cells on the same topography.

b. Two-dimensional variation of bottom depth

The diagonally upward or downward mass fluxes introduced in the previous simple case are generalized for flows over bottom topography that varies two-dimensionally. For simplicity, we consider a two-layer case without losing generality. First, we consider three examples of bottom relief, and then generalize the results.

■Example 1 Consider a case in which all cells are sea cells in the upper and lower layers except for cell **d** in the lower layer (cell $\mathbf{d}_l$) (Figure 7.2). We use suffixes l and u to designate the lower and the upper layer. The central T-point and T-cell are represented by A. The vertical mass flux W^T should be continuous at the interface between cells A_l and A_u, though the area of cell A_l (3/4 measured in grid area units) differs from that of A_u (1 unit). Let us consider how this T-cell mass flux W^T should be distributed to the mass flux W^U of neighboring cells represented by **a**, **b**, **c**, and **d**. In the lower layer, W_T is shared by three cells, $\mathbf{a}_l$, $\mathbf{b}_l$, and $\mathbf{c}_l$, so the contribution of W^T to each W^U is $W^T/3$, but in the upper layer, it is $W^T/4$ because part of W_T should also be shared by W^U at cell $\mathbf{d}_u$. Here W^U at the bottom of cell $\mathbf{d}_u$ is no longer zero. Therefore, $W^T/4$ of the $W^T/3$ shared by each of the three lower sea grid cells $\mathbf{a}_l$, $\mathbf{b}_l$, and $\mathbf{c}_l$ is purely vertical, and the remaining $W^T/12$ (= $W^T/3 - W^T/4$) flows to cell $\mathbf{d}_u$ through the interface. Gathering these diagonal fluxes from the lower three cells, the total amount entering cell $\mathbf{d}_u$ is certainly $W^T/4$ (=$W^T/12 \times 3$). The advected momentum value should be the mean of those at the starting and ending cells of the flux, if the centered difference scheme is used, which is necessary to conserve the total kinetic energy.

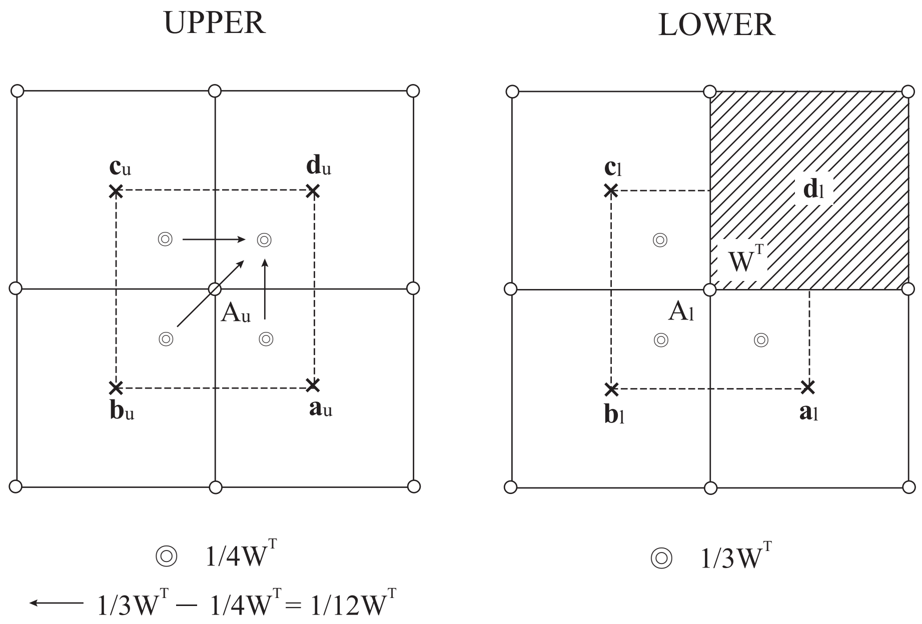

Figure7.2 First example of land-sea patterns, in which all four upper cells are sea cells, with three sea cells and one land cell in the lower layer.

■Example 2 Next, consider an example in which only $\mathbf{b}_l$ is a sea cell in the lower layer, and all four cells are sea cells in the upper layer (Figure 7.3). In the lower layer, W^T is shared only by $\mathbf{b}_l$ but in the upper layer, it is shared by all four cells. Therefore, $W^T/4$ of W^T at cell $\mathbf{b}_l$ is carried vertically upward and the remaining $3W^T/4$ is distributed to the other three cells in the upper layer ($\mathbf{a}_u$, $\mathbf{c}_u$, and $\mathbf{d}_u$), each receiving $W^T/4$.

■Example 3 A third example holds that the upper layer also has land area. In this example, cells $\mathbf{c}_l$, $\mathbf{d}_l$, and $\mathbf{d}_u$ are land cells and the others are sea cells (Figure 7.4). In the lower layer, W^T is shared by two cells ($\mathbf{a}_l$ and $\mathbf{b}_l$) while it is shared by three cells ($\mathbf{a}_u$, $\mathbf{b}_u$, and $\mathbf{c}_u$) in the upper layer. Therefore, from each of $\mathbf{a}_l$ and $\mathbf{b}_l$, $W^T/3$ of $W^T/2$ goes vertically upward and the remaining $W^T/6$ (= $W^T/2 - W^T/3$) goes diagonally upward to cell $\mathbf{c}_u$ with a total amount of $W^T/3$ (= $W^T/6 \times 2$).

c. Generalization

The relationship between the land-sea distribution and the vertically and diagonally upward fluxes stated above is generalized for an arbitrary land-sea distribution. Assume cell $\mathbf{d}_l$ is a land but cell $\mathbf{d}_u$ is a sea cell and consider the diagonally upward fluxes coming to cell $\mathbf{d}_u$. We take N_l as the number of sea cells around point A in the lower layer and N_u as the number in the upper layer ($1 \leq N_l < N_u \leq 4$). Each cell in the lower layer carries W^T/N_l, and W^T/N_u of it goes vertically upward. The remaining

$$W^T/N_l - W^T/N_u = W^T(N_u - N_l)/(N_l N_u) \tag{7.5}$$

should be distributed as diagonally upward fluxes to sea cells in the upper layer at which the lower layer is land. The number of such upper sea cells is $N_u - N_l$ including cell $\mathbf{d}_u$. Thus, each diagonally upward flux coming to cell $\mathbf{d}_u$ is

$$W^T(N_u - N_l)/(N_l N_u) \times 1/(N_u - N_l) = W^T/(N_l N_u). \tag{7.6}$$

The number of such fluxes coming to the cell $\mathbf{d}_u$ is N_l, so their total is

$$W^T/(N_l N_u) \times N_l = W^T/N_u. \tag{7.7}$$

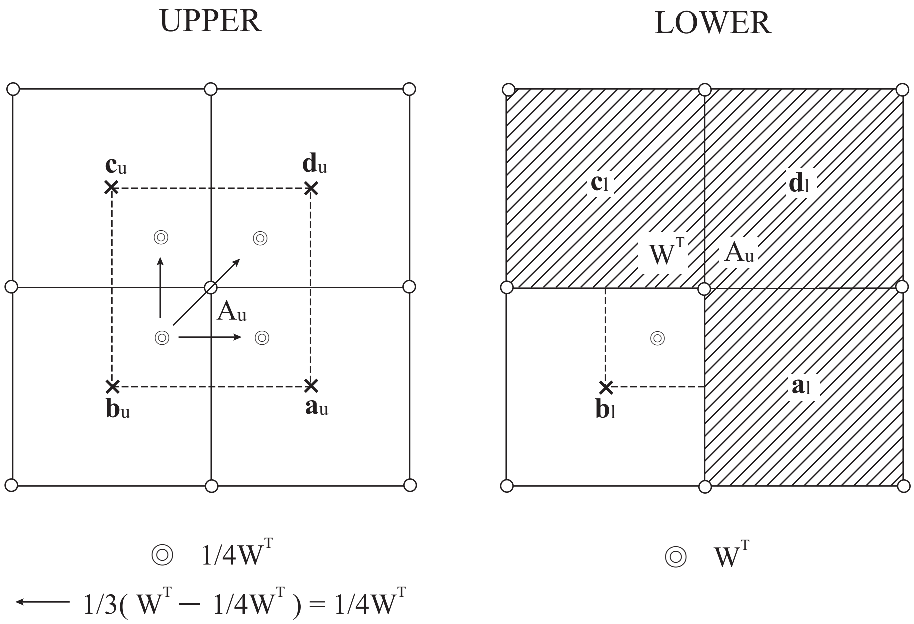

Figure7.3 Second example of land-sea patterns, in which all four upper cells are sea cells, with one sea cell and three land cells in the lower layer.

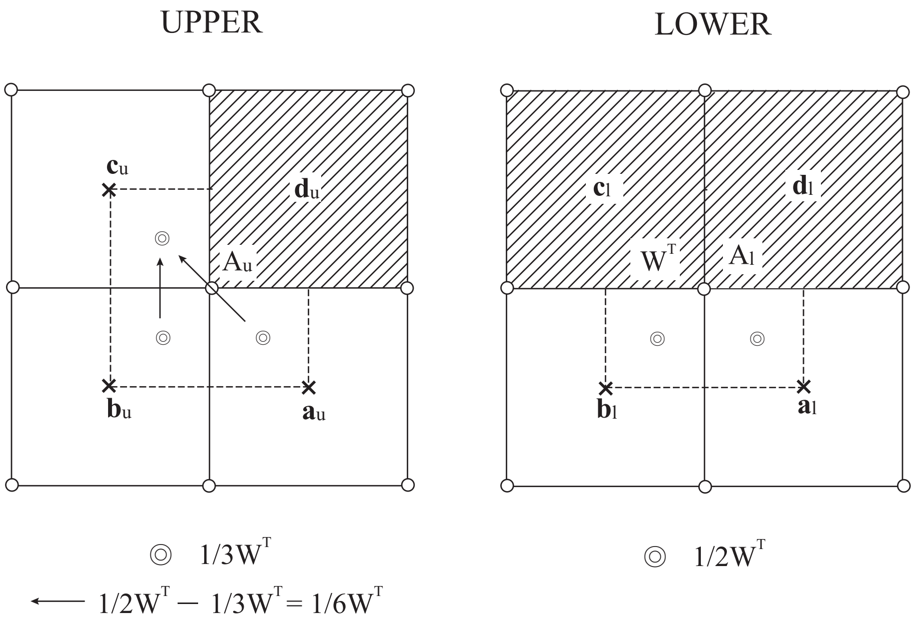

Figure7.4 Third example of land-sea patterns, in which one of the upper cells is a land cell, with two land and two sea cells in the lower layer.

Based on these discussions we understand the difference between (7.3) and (7.4).

We regard the name of each cell such as $\mathbf{a}_l$ also as a land-sea index. If we assume that $\mathbf{a}_l = 1(0)$ when cell $\mathbf{a}_l$ is a sea (land) cell, then the diagonally upward mass flux and momentum flux coming from cell $\mathbf{a}_l$ to cell $\mathbf{d}_u$ are

$$\mathbf{a}_l W^T/(N_l N_u) \quad \text{and} \quad \mathbf{a}_l W^T(u_{\mathrm{a}_l} + u_{\mathrm{d}_u})/(2N_l N_u), \tag{7.8}$$

where u_{a_l} and u_{d_u} are the velocity at cells $\mathbf{a}_l$ and $\mathbf{d}_u$, respectively. Purely vertical mass flux and momentum flux from cell $\mathbf{a}_l$ to cell $\mathbf{a}_u$ are expressed as

$$\mathbf{a}_l W^T/N_u \quad \text{and} \quad \mathbf{a}_l W^T(u_{\mathrm{a}_l} + u_{\mathrm{a}_u})/(2N_u), \tag{7.9}$$

respectively, where u_{a_u} is the velocity at cell $\mathbf{a}_u$. Similar formulations apply to cells $\mathbf{b}_l$ and $\mathbf{c}_l$.

Mass and momentum fluxes for W^T at other T-points around cell $\mathbf{d}_u$ should be calculated similarly to complete vertically and diagonally upward momentum advections around cell $\mathbf{d}_u$. When $N_u = N_l$, diagonally upward fluxes need not be considered and only vertical fluxes (7.9) apply.

To summarize, the discrete expression for the vertical flux of zonal momentum that is transported into a U-cell at $(i+\frac{1}{2}, j+\frac{1}{2}, k-\frac{1}{2})$ through its bottom, $F_{\mathbf{L}_{i+\frac{1}{2},j+\frac{1}{2},k}}(u)$, is given as follows:

$$
\begin{aligned}
F_{\mathbf{L}_{i+\frac{1}{2},j+\frac{1}{2},k}}(u) =& \frac{1}{2}(u_{i+\frac{1}{2},j+\frac{1}{2},k-\frac{1}{2}} + u_{i+\frac{1}{2},j+\frac{1}{2},k+\frac{1}{2}}) \times \left[\frac{W^T_{i,j,k}}{N_{i,j,k-\frac{1}{2}}} + \frac{W^T_{i+1,j,k}}{N_{i+1,j,k-\frac{1}{2}}} + \frac{W^T_{i,j+1,k}}{N_{i,j+1,k-\frac{1}{2}}} + \frac{W^T_{i+1,j+1,k}}{N_{i+1,j+1,k-\frac{1}{2}}} \right] \\
&+ \frac{e_{i+\frac{1}{2},j+\frac{1}{2},k-\frac{1}{2}}(1 - e_{i+\frac{1}{2},j+\frac{1}{2},k+\frac{1}{2}})}{2} \times \\
&\Big[\Big\{ e_{i-\frac{1}{2},j-\frac{1}{2},k+\frac{1}{2}}(u_{i+\frac{1}{2},j+\frac{1}{2},k-\frac{1}{2}} + u_{i-\frac{1}{2},j-\frac{1}{2},k+\frac{1}{2}}) + e_{i+\frac{1}{2},j-\frac{1}{2},k+\frac{1}{2}}(u_{i+\frac{1}{2},j+\frac{1}{2},k-\frac{1}{2}} + u_{i+\frac{1}{2},j-\frac{1}{2},k+\frac{1}{2}}) \\
&+ e_{i-\frac{1}{2},j+\frac{1}{2},k+\frac{1}{2}}(u_{i+\frac{1}{2},j+\frac{1}{2},k-\frac{1}{2}} + u_{i-\frac{1}{2},j+\frac{1}{2},k+\frac{1}{2}}) \Big\} \times \frac{W^T_{i,j,k}}{N_{i,j,k+\frac{1}{2}} N_{i,j,k-\frac{1}{2}}} \\
&+ \Big\{ e_{i+\frac{1}{2},j-\frac{1}{2},k+\frac{1}{2}}(u_{i+\frac{1}{2},j+\frac{1}{2},k-\frac{1}{2}} + u_{i+\frac{1}{2},j-\frac{1}{2},k+\frac{1}{2}}) + e_{i+\frac{3}{2},j-\frac{1}{2},k+\frac{1}{2}}(u_{i+\frac{1}{2},j+\frac{1}{2},k-\frac{1}{2}} + u_{i+\frac{3}{2},j-\frac{1}{2},k+\frac{1}{2}}) \\
&+ e_{i+\frac{3}{2},j+\frac{1}{2},k+\frac{1}{2}}(u_{i+\frac{1}{2},j+\frac{1}{2},k-\frac{1}{2}} + u_{i+\frac{3}{2},j+\frac{1}{2},k+\frac{1}{2}}) \Big\} \times \frac{W^T_{i+1,j,k}}{N_{i+1,j,k+\frac{1}{2}} N_{i+1,j,k-\frac{1}{2}}} \\
&+ \Big\{ e_{i-\frac{1}{2},j+\frac{1}{2},k+\frac{1}{2}}(u_{i+\frac{1}{2},j+\frac{1}{2},k-\frac{1}{2}} + u_{i-\frac{1}{2},j+\frac{1}{2},k+\frac{1}{2}}) + e_{i-\frac{1}{2},j+\frac{3}{2},k+\frac{1}{2}}(u_{i+\frac{1}{2},j+\frac{1}{2},k-\frac{1}{2}} + u_{i-\frac{1}{2},j+\frac{3}{2},k+\frac{1}{2}}) \\
&+ e_{i+\frac{1}{2},j+\frac{3}{2},k+\frac{1}{2}}(u_{i+\frac{1}{2},j+\frac{1}{2},k-\frac{1}{2}} + u_{i+\frac{1}{2},j+\frac{3}{2},k+\frac{1}{2}}) \Big\} \times \frac{W^T_{i,j+1,k}}{N_{i,j+1,k+\frac{1}{2}} N_{i,j+1,k-\frac{1}{2}}} \\
&+ \Big\{ e_{i+\frac{3}{2},j+\frac{1}{2},k+\frac{1}{2}}(u_{i+\frac{1}{2},j+\frac{1}{2},k-\frac{1}{2}} + u_{i+\frac{3}{2},j+\frac{1}{2},k+\frac{1}{2}}) + e_{i+\frac{1}{2},j+\frac{3}{2},k+\frac{1}{2}}(u_{i+\frac{1}{2},j+\frac{1}{2},k-\frac{1}{2}} + u_{i+\frac{1}{2},j+\frac{3}{2},k+\frac{1}{2}}) \\
&+ e_{i+\frac{3}{2},j+\frac{3}{2},k+\frac{1}{2}}(u_{i+\frac{1}{2},j+\frac{1}{2},k-\frac{1}{2}} + u_{i+\frac{3}{2},j+\frac{3}{2},k+\frac{1}{2}}) \Big\} \times \frac{W^T_{i+1,j+1,k}}{N_{i+1,j+1,k+\frac{1}{2}} N_{i+1,j+1,k-\frac{1}{2}}} \Big],
\end{aligned}
\tag{7.10}
$$

where $e_{i+\frac{1}{2},j+\frac{1}{2},k-\frac{1}{2}}$ is the land-sea index for a U-cell (unity for sea and zero for land). Note that diagonally upward/downward momentum fluxes may only occur for a U-cell with the sea floor underneath. The momentum fluxes entering and leaving the cells at the lower level ($k = k + \frac{1}{2}$) are individually added or removed from the cell when calculating them.

7.1.2 Horizontal mass flux and its momentum advection

a. Horizontal mass fluxes

We next consider the generalization of the U-cell horizontal mass fluxes for arbitrary coast lines, in order to derive the horizontal momentum advection. To do this, we start with the generalization of the T-cell mass continuity (5.12)-(5.18). Assuming that $e_{i+\frac{1}{2},j+\frac{1}{2}}$ is a land-sea index (unity for sea and zero for land) for U-cell $(i+\frac{1}{2}, j+\frac{1}{2})$, the general formulae for $U^T_{i+\frac{1}{2},j}$ and $V^T_{i,j+\frac{1}{2}}$ are given as

$$
\begin{aligned}
U^T_{i+\frac{1}{2},j} =& \frac{1}{2}(e_{i+\frac{1}{2},j-\frac{1}{2}} + e_{i+\frac{1}{2},j+\frac{1}{2}}) u^*_{i+\frac{1}{2},j} \Delta y_{i+\frac{1}{2},j} \Delta z \\
&\text{and} \\
V^T_{i,j+\frac{1}{2}} =& \frac{1}{2}(e_{i-\frac{1}{2},j+\frac{1}{2}} + e_{i+\frac{1}{2},j+\frac{1}{2}}) v^*_{i,j+\frac{1}{2}} \Delta x_{i,j+\frac{1}{2}} \Delta z,
\end{aligned}
\tag{7.11}
$$

where, $u^*_{i+\frac{1}{2},j}$ and $v^*_{i,j+\frac{1}{2}}$ are the zonal and meridional velocity at the eastern and northern side boundary of a T-cell (i, j) as computed by (5.14), (5.16), and (5.18). Here we neglect the vertical subscript $(k-\frac{1}{2})$.

Substituting these formulae into the T-cell mass continuity (5.12), the X (zonal) component of the mass continuity for

U-cell $(i+\frac{1}{2}, j+\frac{1}{2})$ (5.21), $\mathrm{XMC}^U_{i+\frac{1}{2},j+\frac{1}{2}}$, multiplied by its own land-sea signature $e_{i+\frac{1}{2},j+\frac{1}{2}}$, is expressed as

$$\begin{aligned}
\mathrm{XMC}^U_{i+\frac{1}{2},j+\frac{1}{2}} &= e_{i+\frac{1}{2},j+\frac{1}{2}} \frac{\Delta y_{i+\frac{1}{2},j+\frac{1}{2}}}{2} \Delta z \\
&\times \Big\{ \frac{1}{N_{i,j}} [(e_{i-\frac{1}{2},j-\frac{1}{2}} + e_{i-\frac{1}{2},j+\frac{1}{2}}) u^*_{i-\frac{1}{2},j} - (e_{i+\frac{1}{2},j-\frac{1}{2}} + e_{i+\frac{1}{2},j+\frac{1}{2}}) u^*_{i+\frac{1}{2},j}] \\
&+ \frac{1}{N_{i+1,j}} [(e_{i+\frac{1}{2},j-\frac{1}{2}} + e_{i+\frac{1}{2},j+\frac{1}{2}}) u^*_{i+\frac{1}{2},j} - (e_{i+\frac{3}{2},j-\frac{1}{2}} + e_{i+\frac{3}{2},j+\frac{1}{2}}) u^*_{i+\frac{3}{2},j}] \\
&+ \frac{1}{N_{i,j+1}} [(e_{i-\frac{1}{2},j+\frac{1}{2}} + e_{i-\frac{1}{2},j+\frac{3}{2}}) u^*_{i-\frac{1}{2},j+1} - (e_{i+\frac{1}{2},j+\frac{1}{2}} + e_{i+\frac{1}{2},j+\frac{3}{2}}) u^*_{i+\frac{1}{2},j+1}] \\
&+ \frac{1}{N_{i+1,j+1}} [(e_{i+\frac{1}{2},j+\frac{1}{2}} + e_{i+\frac{1}{2},j+\frac{3}{2}}) u^*_{i+\frac{1}{2},j+1} - (e_{i+\frac{3}{2},j+\frac{1}{2}} + e_{i+\frac{3}{2},j+\frac{3}{2}}) u^*_{i+\frac{3}{2},j+1}] \Big\} \\
&= e_{i+\frac{1}{2},j+\frac{1}{2}} \frac{\Delta y_{i+\frac{1}{2},j+\frac{1}{2}}}{2} \Delta z \times \Big\{ \Big[\frac{1}{N_{i,j}} (e_{i-\frac{1}{2},j-\frac{1}{2}} + e_{i-\frac{1}{2},j+\frac{1}{2}}) u^*_{i-\frac{1}{2},j} \\
&+ \Big(-\frac{1}{N_{i,j}} + \frac{1}{N_{i+1,j}} \Big) (e_{i+\frac{1}{2},j-\frac{1}{2}} + e_{i+\frac{1}{2},j+\frac{1}{2}}) u^*_{i+\frac{1}{2},j} \\
&- \frac{1}{N_{i+1,j}} (e_{i+\frac{3}{2},j-\frac{1}{2}} + e_{i+\frac{3}{2},j+\frac{1}{2}}) u^*_{i+\frac{3}{2},j} \Big] \\
&+ \Big[\frac{1}{N_{i,j+1}} (e_{i-\frac{1}{2},j+\frac{1}{2}} + e_{i-\frac{1}{2},j+\frac{3}{2}}) u^*_{i-\frac{1}{2},j+1} \\
&+ \Big(-\frac{1}{N_{i,j+1}} + \frac{1}{N_{i+1,j+1}} \Big) (e_{i+\frac{1}{2},j+\frac{1}{2}} + e_{i+\frac{1}{2},j+\frac{3}{2}}) u^*_{i+\frac{1}{2},j+1} \\
&- \frac{1}{N_{i+1,j+1}} (e_{i+\frac{3}{2},j+\frac{1}{2}} + e_{i+\frac{3}{2},j+\frac{3}{2}}) u^*_{i+\frac{3}{2},j+1} \Big] \Big\}.
\end{aligned} \tag{7.12}$$

Here, recalling

$$N_{i,j} = e_{i-\frac{1}{2},j-\frac{1}{2}} + e_{i+\frac{1}{2},j-\frac{1}{2}} + e_{i-\frac{1}{2},j+\frac{1}{2}} + e_{i+\frac{1}{2},j+\frac{1}{2}}, \tag{7.13}$$

we have,

$$\begin{aligned}
&\Big(-\frac{1}{N_{i,j}} + \frac{1}{N_{i+1,j}} \Big) (e_{i+\frac{1}{2},j-\frac{1}{2}} + e_{i+\frac{1}{2},j+\frac{1}{2}}) \\
&\qquad = \frac{1}{N_{i,j}} (e_{i-\frac{1}{2},j-\frac{1}{2}} + e_{i-\frac{1}{2},j+\frac{1}{2}}) - \frac{1}{N_{i+1,j}} (e_{i+\frac{3}{2},j-\frac{1}{2}} + e_{i+\frac{3}{2},j+\frac{1}{2}})
\end{aligned} \tag{7.14}$$

and

$$\begin{aligned}
&\Big(-\frac{1}{N_{i,j+1}} + \frac{1}{N_{i+1,j+1}} \Big) (e_{i+\frac{1}{2},j+\frac{1}{2}} + e_{i+\frac{1}{2},j+\frac{3}{2}}) \\
&\qquad = \frac{1}{N_{i,j+1}} (e_{i-\frac{1}{2},j+\frac{1}{2}} + e_{i-\frac{1}{2},j+\frac{3}{2}}) - \frac{1}{N_{i+1,j+1}} (e_{i+\frac{3}{2},j+\frac{1}{2}} + e_{i+\frac{3}{2},j+\frac{3}{2}}).
\end{aligned} \tag{7.15}$$

Thus, based on (5.24) and (5.25),

$$
\begin{aligned}
\mathrm{XMC}^{U}_{i+\frac{1}{2},j+\frac{1}{2}} &= e_{i+\frac{1}{2},j+\frac{1}{2}} \frac{\Delta y_{i+\frac{1}{2},j+\frac{1}{2}}}{2} \Delta z \Big\{ \Big[\frac{1}{N_{i,j}} (e_{i-\frac{1}{2},j-\frac{1}{2}} + e_{i-\frac{1}{2},j+\frac{1}{2}})(u^{*}_{i-\frac{1}{2},j} + u^{*}_{i+\frac{1}{2},j}) \\
&\quad - \frac{1}{N_{i+1,j}} (e_{i+\frac{3}{2},j-\frac{1}{2}} + e_{i+\frac{3}{2},j+\frac{1}{2}})(u^{*}_{i+\frac{1}{2},j} + u^{*}_{i+\frac{3}{2},j}) \Big] \\
&\quad + \Big[\frac{1}{N_{i,j+1}} (e_{i-\frac{1}{2},j+\frac{1}{2}} + e_{i-\frac{1}{2},j+\frac{3}{2}})(u^{*}_{i-\frac{1}{2},j+1} + u^{*}_{i+\frac{1}{2},j+1}) \\
&\quad - \frac{1}{N_{i+1,j+1}} (e_{i+\frac{3}{2},j+\frac{1}{2}} + e_{i+\frac{3}{2},j+\frac{3}{2}})(u^{*}_{i+\frac{1}{2},j+1} + u^{*}_{i+\frac{3}{2},j+1}) \Big] \Big\} \\
&= e_{i+\frac{1}{2},j+\frac{1}{2}} \Big[e_{i-\frac{1}{2},j+\frac{1}{2}} \Big(\frac{1}{N_{i,j}} U^{U}_{i,j} + \frac{1}{N_{i,j+1}} U^{U}_{i,j+1} \Big) \\
&\quad - e_{i+\frac{3}{2},j+\frac{1}{2}} \Big(\frac{1}{N_{i+1,j}} U^{U}_{i+1,j} + \frac{1}{N_{i+1,j+1}} U^{U}_{i+1,j+1} \Big) + e_{i-\frac{1}{2},j-\frac{1}{2}} \frac{1}{N_{i,j}} U^{U}_{i,j} \\
&\quad - e_{i+\frac{3}{2},j+\frac{3}{2}} \frac{1}{N_{i+1,j+1}} U^{U}_{i+1,j+1} + e_{i-\frac{1}{2},j+\frac{3}{2}} \frac{1}{N_{i,j+1}} U^{U}_{i,j+1} - e_{i+\frac{3}{2},j-\frac{1}{2}} \frac{1}{N_{i+1,j}} U^{U}_{i+1,j} \Big].
\end{aligned}
\tag{7.16}
$$

Adding the Y (meridional) component, YMC (the expression is omitted here), to the above formula, we obtain the horizontal part of the U-cell mass continuity, HMC, as follows:

$$
\begin{aligned}
\mathrm{HMC}^{U}_{i+\frac{1}{2},j+\frac{1}{2}} &= \mathrm{XMC}^{U}_{i+\frac{1}{2},j+\frac{1}{2}} + \mathrm{YMC}^{U}_{i+\frac{1}{2},j+\frac{1}{2}} \\
&= e_{i+\frac{1}{2},j+\frac{1}{2}} \\
&\times \Big[e_{i-\frac{1}{2},j+\frac{1}{2}} \Big(\frac{1}{N_{i,j}} U^{U}_{i,j} + \frac{1}{N_{i,j+1}} U^{U}_{i,j+1} \Big) - e_{i+\frac{3}{2},j+\frac{1}{2}} \Big(\frac{1}{N_{i+1,j}} U^{U}_{i+1,j} + \frac{1}{N_{i+1,j+1}} U^{U}_{i+1,j+1} \Big) \\
&+ e_{i+\frac{1}{2},j-\frac{1}{2}} \Big(\frac{1}{N_{i,j}} V^{U}_{i,j} + \frac{1}{N_{i+1,j}} V^{U}_{i+1,j} \Big) - e_{i+\frac{1}{2},j+\frac{3}{2}} \Big(\frac{1}{N_{i,j+1}} V^{U}_{i,j+1} + \frac{1}{N_{i+1,j+1}} V^{U}_{i+1,j+1} \Big) \\
&+ e_{i-\frac{1}{2},j-\frac{1}{2}} \frac{1}{N_{i,j}} (U^{U}_{i,j} + V^{U}_{i,j}) - e_{i+\frac{3}{2},j+\frac{3}{2}} \frac{1}{N_{i+1,j+1}} (U^{U}_{i+1,j+1} + V^{U}_{i+1,j+1}) \\
&+ e_{i-\frac{1}{2},j+\frac{3}{2}} \frac{1}{N_{i,j+1}} (U^{U}_{i,j+1} - V^{U}_{i,j+1}) - e_{i+\frac{3}{2},j-\frac{1}{2}} \frac{1}{N_{i+1,j}} (U^{U}_{i+1,j} - V^{U}_{i+1,j}) \Big].
\end{aligned}
\tag{7.17}
$$

Assuming mass fluxes $M_{\mathbf{E}}$, $M_{\mathbf{N}}$, $M_{\mathbf{NE}}$, $M_{\mathbf{SE}}$ as follows:

$$
\begin{aligned}
M_{\mathbf{E}_{i,j+\frac{1}{2}}} &= e_{i+\frac{1}{2},j+\frac{1}{2}} e_{i-\frac{1}{2},j+\frac{1}{2}} \Big(\frac{1}{N_{i,j}} U^{U}_{i,j} + \frac{1}{N_{i,j+1}} U^{U}_{i,j+1} \Big), \\
M_{\mathbf{N}_{i+\frac{1}{2},j}} &= e_{i+\frac{1}{2},j+\frac{1}{2}} e_{i+\frac{1}{2},j-\frac{1}{2}} \Big(\frac{1}{N_{i,j}} V^{U}_{i,j} + \frac{1}{N_{i+1,j}} V^{U}_{i+1,j} \Big), \\
M_{\mathbf{NE}_{i,j}} &= e_{i+\frac{1}{2},j+\frac{1}{2}} e_{i-\frac{1}{2},j-\frac{1}{2}} \frac{1}{N_{i,j}} (U^{U}_{i,j} + V^{U}_{i,j}), \\
M_{\mathbf{SE}_{i,j}} &= e_{i-\frac{1}{2},j+\frac{1}{2}} e_{i+\frac{1}{2},j-\frac{1}{2}} \frac{1}{N_{i,j}} (U^{U}_{i,j} - V^{U}_{i,j}),
\end{aligned}
\tag{7.18}
$$

then,

$$
\begin{aligned}
\mathrm{HMC}^{U}_{i+\frac{1}{2},j+\frac{1}{2}} =& M_{\mathbf{E}_{i,j+\frac{1}{2}}} - M_{\mathbf{E}_{i+1,j+\frac{1}{2}}} + M_{\mathbf{N}_{i+\frac{1}{2},j}} - M_{\mathbf{N}_{i+\frac{1}{2},j+1}} \\
&+ M_{\mathbf{NE}_{i,j}} - M_{\mathbf{NE}_{i+1,j+1}} + M_{\mathbf{SE}_{i,j+1}} - M_{\mathbf{SE}_{i+1,j}}.
\end{aligned}
\tag{7.19}
$$

Here, $M_{\mathbf{E}}$ and $M_{\mathbf{N}}$ are axis-parallel mass fluxes, and $M_{\mathbf{NE}}$ and $M_{\mathbf{SE}}$ are horizontally diagonal ones (Figure 7.5).

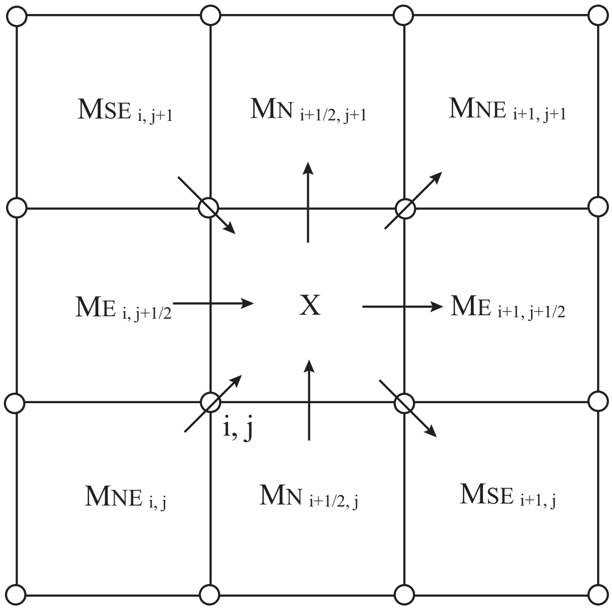

Figure7.5 Distribution of generalized mass fluxes for U-cell $(i+1/2, j+1/2)$

If we derive the formula for the standard case from (7.17) (all of N are 4),

$$\begin{aligned}
\mathrm{HMC}^{U}_{i+\frac{1}{2},j+\frac{1}{2}} = \frac{1}{2} & \Big[\frac{1}{2}(U^U_{i,j} + U^U_{i,j+1}) - \frac{1}{2}(U^U_{i+1,j} + U^U_{i+1,j+1}) \\
& + \frac{1}{2}(V^U_{i,j} + V^U_{i,j+1}) - \frac{1}{2}(V^U_{i+1,j} + V^U_{i+1,j+1})\Big] \\
+\frac{1}{2} & \Big[\frac{1}{2}(U^U_{i,j} + V^U_{i,j}) - \frac{1}{2}(U^U_{i+1,j+1} + V^U_{i+1,j+1}) \\
& + \frac{1}{2}(U^U_{i,j+1} - V^U_{i,j+1}) - \frac{1}{2}(U^U_{i+1,j} - V^U_{i+1,j})\Big].
\end{aligned} \tag{7.20}$$

This expression means that the horizontal mass flux convergence is a mean of those of the axis-parallel mass fluxes (5.23) and of the diagonal ones (5.28). However, their weighting factors α and β are both $1/2$ in the present case, while $(\alpha, \beta) = (2/3, 1/3)$ for the generalized Arakawa scheme, which conserves quasi-enstrophy such as $(\delta v/\delta x)^2$ and $(\delta u/\delta y)^2$ in a horizontally non-divergent flow.

b. Horizontal momentum advection

For the standard case away from land, we have the freedom to choose weights $(\alpha : \beta)$ for averaging the convergences of the axis-parallel and the horizontally diagonal mass fluxes, as long as $\alpha + \beta = 1$, as seen in (7.20). In MRI.COM $\alpha = 2/3$ and $\beta = 1/3$ are chosen for the standard case so that the momentum advection terms lead to the generalized Arakawa scheme. In this case the zonal momentum advection term is expressed by convergence of the horizontal momentum fluxes

Table7.1 Definition of a land-sea index, the index identifying each case (column **A**), the coefficient of $U^U_{i,j}$ in the axis-parallel mass flux (column **B**), and the coefficient of $U^U_{i,j}$ in the horizontally diagonal mass flux (column **C**), for eight combinations of indices **a**, **b**, and **c** in Figure 7.2b (see the main text). Cell **d** is assumed to be a sea cell, and the momentum advection by means of $U^U_{i,j}$ into and from cell **d** is generalized. Note that $U^U_{i,j}$ is identically zero for cases 5 and 8 (**b** = **c** = 0).

CASE n	Land-sea index **a**	 **b**	 **c**	**A**	**B** Coefficient of $U^U_{i,j}$ (axis-parallel) +	**C** Coefficient of $U^U_{i,j}$ (horizontally-diagonal) ×
1	1	1	1	**abc**	1/3	1/6
2	1	1	0	**ab**(1 − **c**)	0	1/3
3	1	0	1	**ab**(1 − **b**)**c**	1/3	0
4	0	1	1	(1 − **a**)**bc**	1/3	1/3
5	1	0	0	–	0	0
6	0	1	0	(1 − **a**)**b**(1 − **c**)	0	1/2
7	0	0	1	(1 − **a**)(1 − **b**)**c**	1/2	0
8	0	0	0	–	0	0

as follows:

$$\begin{aligned}
\mathrm{CAD}_{i+\frac{1}{2},j+\frac{1}{2}}(u) = \frac{2}{3}\Big[&\frac{1}{2}(u_{i-\frac{1}{2},j+\frac{1}{2}} + u_{i+\frac{1}{2},j+\frac{1}{2}})\frac{1}{2}(U^U_{i,j} + U^U_{i,j+1}) \\
&- \frac{1}{2}(u_{i+\frac{1}{2},j+\frac{1}{2}} + u_{i+\frac{3}{2},j+\frac{1}{2}})\frac{1}{2}(U^U_{i+1,j} + U^U_{i+1,j+1}) \\
&+ \frac{1}{2}(u_{i+\frac{1}{2},j-\frac{1}{2}} + u_{i+\frac{1}{2},j+\frac{1}{2}})\frac{1}{2}(V^U_{i,j} + V^U_{i+1,j}) \\
&- \frac{1}{2}(u_{i+\frac{1}{2},j+\frac{1}{2}} + u_{i+\frac{1}{2},j+\frac{3}{2}})\frac{1}{2}(V^U_{i,j+1} + V^U_{i+1,j+1})\Big] \\
+\frac{1}{3}\Big[&\frac{1}{2}(u_{i+\frac{1}{2},j+\frac{1}{2}} + u_{i-\frac{1}{2},j-\frac{1}{2}})\frac{1}{2}(U^U_{i,j} + V^U_{i,j}) \\
&- \frac{1}{2}(u_{i+\frac{1}{2},j+\frac{1}{2}} + u_{i+\frac{3}{2},j+\frac{3}{2}})\frac{1}{2}(U^U_{i+1,j+1} + V^U_{i+1,j+1}) \\
&+ \frac{1}{2}(u_{i+\frac{1}{2},j+\frac{1}{2}} + u_{i-\frac{1}{2},j+\frac{3}{2}})\frac{1}{2}(U^U_{i,j+1} - V^U_{i,j+1}) \\
&- \frac{1}{2}(u_{i+\frac{1}{2},j+\frac{1}{2}} + u_{i+\frac{3}{2},j-\frac{1}{2}})\frac{1}{2}(U^U_{i+1,j} - V^U_{i+1,j})\Big]
\end{aligned} \tag{7.21}$$

This scheme under Arakawa's B-grid arrangement conserves the quasi-enstrophies ($(\partial u/\partial y)^2$ and $(\partial v/\partial x)^2$) in a horizontally non-divergent flow.

To merge the generalized Arakawa scheme for the standard case into the general form of the horizontal mass flux expressed in Figure 7.5 and related momentum flux, let us examine the axis-parallel and horizontally diagonal mass flux associated with $U^U_{i,j}$, taking topography into account. Look at Figure 7.2b, where letters **a**, **b**, **c**, and **d** designate the land-sea index and names of U-cells. Cell **d** is assumed to be a sea cell (**d** = 1). We analyze two kinds of mass fluxes associated with $U^U_{i,j}$ under different combinations of **a**, **b**, and **c** (eight cases), as indicated in the first column in Table 7.1. Column (A) corresponds to an index, which is unity for its own combination and zero for all other combinations. Column (B) lists the coefficient of $U^U_{i,j}$ in the axis-parallel mass flux of the U-cell mass continuity (7.17). Column (C) indicates the coefficient of $U^U_{i,j}$ in the horizontally diagonal mass flux of (7.17).

The generalized coefficient of $U^U_{i,j}$ in the axis-parallel mass flux (c_1) is obtained by summing the product of **A** and **B** over the eight cases. Similarly, the generalized coefficient in the horizontally diagonal mass flux (c_2) is obtained by the summing the product of **A** and **C**. That is,

$$c_1 = \sum_{n=1}^{8} \mathbf{A}_n \mathbf{B}_n = \frac{1}{6}\mathbf{c}(\mathbf{ab} - \mathbf{a} - \mathbf{b}+3)$$

and

$$c_2 = \sum_{n=1}^{8} \mathbf{A}_n \mathbf{C}_n = \frac{1}{6}\mathbf{b}(3-\mathbf{a} - \mathbf{c}). \tag{7.22}$$

Then, the axis-parallel and the horizontally diagonal flux of zonal momentum (u) related with $U^U_{i,j}$, multiplied by the land-sea index **d**, are

$$\frac{\mathbf{d}}{2}(u_\mathbf{c} + u_\mathbf{d})c_1 U^U_{i,j} = \frac{1}{2}(u_\mathbf{c} + u_\mathbf{d})\frac{1}{6}\mathbf{cd}(\mathbf{ab} - \mathbf{a} - \mathbf{b}+3)U^U_{i,j},$$

and

$$\frac{\mathbf{d}}{2}(u_\mathbf{b} + u_\mathbf{d})c_2 U^U_{i,j} = \frac{1}{2}(u_\mathbf{b} + u_\mathbf{d})\frac{1}{6}\mathbf{bd}(3-\mathbf{a} - \mathbf{c})U^U_{i,j}, \tag{7.23}$$

respectively.

The resultant momentum fluxes are as follows:

$$\begin{aligned}
F_{\mathbf{E}_{i,j+\frac{1}{2}}}(u) &= \frac{1}{2}(u_{i-\frac{1}{2},j+\frac{1}{2}} + u_{i+\frac{1}{2},j+\frac{1}{2}})M_{\mathbf{E}_{i,j+\frac{1}{2}}},\\
F_{\mathbf{N}_{i+\frac{1}{2},j}}(u) &= \frac{1}{2}(u_{i+\frac{1}{2},j-\frac{1}{2}} + u_{i+\frac{1}{2},j+\frac{1}{2}})M_{\mathbf{N}_{i+\frac{1}{2},j}},\\
F_{\mathbf{NE}_{i,j}}(u) &= \frac{1}{2}(u_{i+\frac{1}{2},j+\frac{1}{2}} + u_{i-\frac{1}{2},j-\frac{1}{2}})M_{\mathbf{NE}_{i,j}},\\
F_{\mathbf{SE}_{i,j}}(u) &= \frac{1}{2}(u_{i-\frac{1}{2},j+\frac{1}{2}} + u_{i+\frac{1}{2},j-\frac{1}{2}})M_{\mathbf{SE}_{i,j}},
\end{aligned} \tag{7.24}$$

where

$$\begin{aligned}
M_{\mathbf{E}_{i,j+\frac{1}{2}}} &= \frac{1}{6}(C_{\mathbf{XN}_{i,j}} U^U_{i,j} + C_{\mathbf{XS}_{i,j+1}} U^U_{i,j+1}),\\
M_{\mathbf{N}_{i+\frac{1}{2},j}} &= \frac{1}{6}(C_{\mathbf{YE}_{i,j}} V^U_{i,j} + C_{\mathbf{YW}_{i+1,j}} V^U_{i+1,j}),\\
M_{\mathbf{NE}_{i,j}} &= \frac{1}{6}C_{\mathbf{NE}_{i,j}}(U^U_{i,j} + V^U_{i,j}),\\
M_{\mathbf{SE}_{i,j}} &= \frac{1}{6}C_{\mathbf{SE}_{i,j}}(U^U_{i,j} - V^U_{i,j}),
\end{aligned} \tag{7.25}$$

and

$$\begin{aligned}
C_{\mathbf{XN}_{i,j}} &= e_{i+\frac{1}{2},j+\frac{1}{2}} e_{i-\frac{1}{2},j+\frac{1}{2}} (e_{i+\frac{1}{2},j-\frac{1}{2}} e_{i-\frac{1}{2},j-\frac{1}{2}} - e_{i+\frac{1}{2},j-\frac{1}{2}} - e_{i-\frac{1}{2},j-\frac{1}{2}} + 3),\\
C_{\mathbf{XS}_{i,j}} &= e_{i+\frac{1}{2},j-\frac{1}{2}} e_{i-\frac{1}{2},j-\frac{1}{2}} (e_{i+\frac{1}{2},j+\frac{1}{2}} e_{i-\frac{1}{2},j+\frac{1}{2}} - e_{i+\frac{1}{2},j+\frac{1}{2}} - e_{i-\frac{1}{2},j+\frac{1}{2}} + 3),\\
C_{\mathbf{YE}_{i,j}} &= e_{i+\frac{1}{2},j+\frac{1}{2}} e_{i+\frac{1}{2},j-\frac{1}{2}} (e_{i-\frac{1}{2},j+\frac{1}{2}} e_{i-\frac{1}{2},j-\frac{1}{2}} - e_{i-\frac{1}{2},j+\frac{1}{2}} - e_{i-\frac{1}{2},j-\frac{1}{2}} + 3),\\
C_{\mathbf{YW}_{i,j}} &= e_{i-\frac{1}{2},j+\frac{1}{2}} e_{i-\frac{1}{2},j-\frac{1}{2}} (e_{i+\frac{1}{2},j+\frac{1}{2}} e_{i+\frac{1}{2},j-\frac{1}{2}} - e_{i+\frac{1}{2},j+\frac{1}{2}} - e_{i+\frac{1}{2},j-\frac{1}{2}} + 3),\\
C_{\mathbf{NE}_{i,j}} &= e_{i+\frac{1}{2},j+\frac{1}{2}} e_{i-\frac{1}{2},j-\frac{1}{2}} (3 - e_{i-\frac{1}{2},j+\frac{1}{2}} - e_{i+\frac{1}{2},j-\frac{1}{2}}),\\
C_{\mathbf{SE}_{i,j}} &= e_{i-\frac{1}{2},j+\frac{1}{2}} e_{i+\frac{1}{2},j-\frac{1}{2}} (3 - e_{i+\frac{1}{2},j+\frac{1}{2}} - e_{i-\frac{1}{2},j-\frac{1}{2}}).
\end{aligned} \tag{7.26}$$

Finally, convergence of the horizontal momentum fluxes is written as

$$\begin{aligned}
\mathrm{CAD}_{i+\frac{1}{2},j+\frac{1}{2}}(u) =& F_{\mathbf{E}_{i,j+\frac{1}{2}}}(u) - F_{\mathbf{E}_{i+1,j+\frac{1}{2}}}(u) + F_{\mathbf{N}_{i+\frac{1}{2},j}}(u) - F_{\mathbf{N}_{i+\frac{1}{2},j+1}}(u)\\
&+ F_{\mathbf{NE}_{i,j}}(u) - F_{\mathbf{NE}_{i+1,j+1}}(u) + F_{\mathbf{SE}_{i,j+1}}(u) - F_{\mathbf{SE}_{i+1,j}}(u).
\end{aligned} \tag{7.27}$$

This is the discrete expression for the advection term of the zonal momentum $\frac{1}{h_\mu h_\psi}\left\{\frac{\partial(z_s h_\psi uu)}{\partial\mu} + \frac{\partial(z_s h_\mu vu)}{\partial\psi}\right\}$ under the finite volume method (equations being integrated over a U-cell).

7.2 Pressure gradient term

In the split-explicit solution method, the pressure gradient term of the horizontal momentum equation is separated into barotropic (fast) and baroclinic (slow) terms (Eq. 2.58). Its form is

$$\underbrace{\frac{1}{\rho_0}\nabla_s(p_a+g\rho_0\eta)}_{\text{fast}}+\underbrace{\overbrace{\frac{1}{\rho_0}\nabla_s\left[g\int_{z(s)}^{\eta}\rho' dz\right]}^{\text{pressure perturbation}}+\overbrace{\frac{g\rho'}{\rho_0}\nabla_s z}^{\text{geopotential}}}_{\text{slow}}\,. \tag{7.28}$$

Here, we use symbol s to indicate z^* for brevity, and so ∇_s means ∇_{z^*}. These three terms correspond to the first, second, and third terms in the r.h.s. of (7.1) and (7.2). From the perspective of the momentum conservation, the finite difference of the pressure gradient terms should be expressed so that the pressure at the interface of adjacent cells is common, giving only boundary pressures after horizontal integration. This is not difficult for the barotropic mode. The baroclinic mode should be considered carefully. Among the baroclinic terms in (7.28), the former is called the pressure perturbation term and the latter is called the geopotential term.

Because sea-floor depth is defined at U-cells in MRI.COM, it is not necessary to consider the horizontal gradient of the sea floor in calculating the pressure gradient for a bottom U-cell unlike σ-coordinate models and possibly the depth-coordinate models that employ staggered grid arrangements different from MRI.COM. This makes the finite difference expression simple, and the pressure gradient error may be expected to be small. However, this simplicity does not hold for the bottom boundary layer (BBL). The treatment of the pressure gradient term for BBL is explained in Chapter 16.

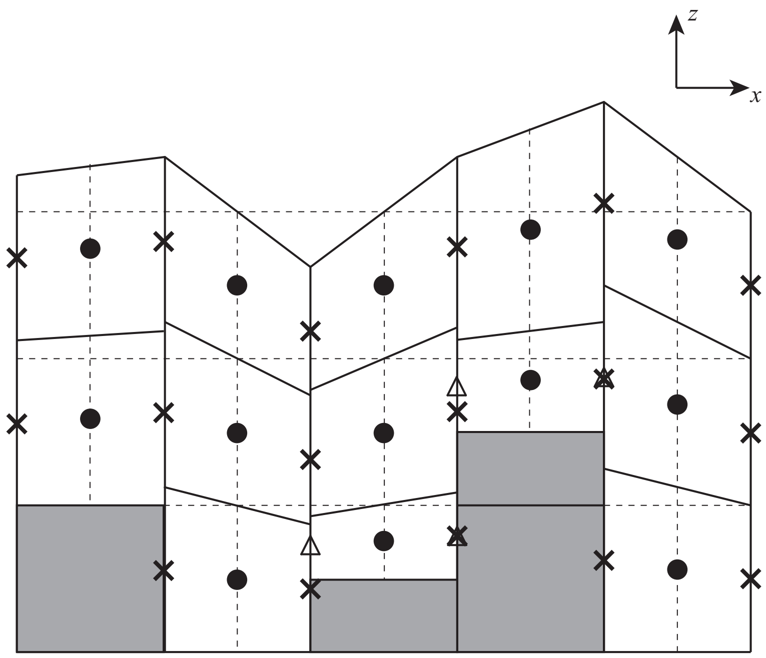

Figure7.6 Illustration of a vertical slice through a set of grid cells in the x-z plane for z^* coordinate. The center point in each cell (•) is a velocity point, and the pressure gradient term is calculated at this point. The cross (×) is a tracer point, and pressure is calculated here. The triangle (△), whose z^* value is that of the adjacent U-point of the bottom U-cell, is the hydrostatic pressure point which is used to evaluate pressure gradient for the bottom U-cell.

a. Discretization of the pressure perturbation term

Figure 7.6 shows the grid points on the x-z plane relevant to calculating pressure gradient terms. Pressures are defined on T-points. Because the actual vertical integration distances are different between adjacent T-points for z^* coordinate, it is appropriate to differentiate pressures after computing them at T-points rather than vertically integrating the pressure gradient as in z coordinate. However, the round-off error due to the differentiation of vertically integrated quantity would increase with depth. To avoid this, we add contribution from the integration over one vertical grid to the pressure gradient term at the upper vertical level, as explained below.

Introducing pressure perturbation p', the pressure perturbation term in Eq. (7.28) is expressed as

$$\frac{1}{\rho_0}\nabla_s\left[g\int_{z(s)}^{\eta}\rho' dz\right]=\frac{1}{\rho_0}\nabla_s p', \tag{7.29}$$

$$\text{where}\quad p'=g\int_{z(s)}^{\eta}\rho' dz. \tag{7.30}$$

A simple discrete expression would be given as follows ($1/\rho_0$ is omitted):

$$(\nabla_s p')_{i+\frac{1}{2},j+\frac{1}{2},k-\frac{1}{2}}=\hat{\mathbf{x}}\frac{\frac{p'_{i+1,j+1,k-\frac{1}{2}}+p'_{i+1,j,k-\frac{1}{2}}}{2}-\frac{p'_{i,j+1,k-\frac{1}{2}}+p'_{i,j,k-\frac{1}{2}}}{2}}{\Delta x_{i+\frac{1}{2},j+\frac{1}{2}}}+\hat{\mathbf{y}}\frac{\frac{p'_{i+1,j+1,k-\frac{1}{2}}+p'_{i,j+1,k-\frac{1}{2}}}{2}-\frac{p'_{i+1,j,k-\frac{1}{2}}+p'_{i,j,k-\frac{1}{2}}}{2}}{\Delta y_{i+\frac{1}{2},j+\frac{1}{2}}}, \tag{7.31}$$

$$\text{where}\quad p'_{i,j,k-\frac{1}{2}}=g\sum_{l=1}^{k-1}(\rho')_{i,j,l-\frac{1}{2}}(\mathtt{dzt})_{i,j,l-\frac{1}{2}}+g(\rho')_{i,j,k-\frac{1}{2}}\frac{(\mathtt{dzt})_{i,j,k-\frac{1}{2}}}{2}. \tag{7.32}$$

However, because density perturbation (ρ') would generally take similar values in adjacent grids, the pressure perturbation (p') would also take similar values in adjacent grids. The round-off error caused by differentiation would increase with the depth. To avoid this round-off error, we use another discrete expression given as follows:

$$\begin{aligned}(\nabla_s p')_{i+\frac{1}{2},j+\frac{1}{2},k-\frac{1}{2}} &= (\nabla_s p')_{i+\frac{1}{2},j+\frac{1}{2},k-\frac{3}{2}}+\left\{(\nabla_s p')_{i+\frac{1}{2},j+\frac{1}{2},k-\frac{1}{2}}-(\nabla_s p')_{i+\frac{1}{2},j+\frac{1}{2},k-\frac{3}{2}}\right\}\\ &= (\nabla_s p')_{i+\frac{1}{2},j+\frac{1}{2},k-\frac{3}{2}}+\hat{\mathbf{x}}\frac{\frac{\Delta p'_{i+1,j+1,k-1}+\Delta p'_{i+1,j,k-1}}{2}-\frac{\Delta p'_{i,j+1,k-1}+\Delta p'_{i,j,k-1}}{2}}{\Delta x_{i+\frac{1}{2},j+\frac{1}{2}}}\\ &\quad+\hat{\mathbf{y}}\frac{\frac{\Delta p'_{i+1,j+1,k-1}+\Delta p'_{i,j+1,k-1}}{2}-\frac{\Delta p'_{i+1,j,k-1}+\Delta p'_{i,j,k-1}}{2}}{\Delta y_{i+\frac{1}{2},j+\frac{1}{2}}},\end{aligned} \tag{7.33}$$

where

$$\Delta p'_{i,j,k-1}\equiv p'_{i,j,k-\frac{1}{2}}-p'_{i,j,k-\frac{3}{2}}=g(\rho')_{i,j,k-\frac{3}{2}}\frac{(\mathtt{dzt})_{i,j,k-\frac{1}{2}}}{2}+g(\rho')_{i,j,k-\frac{1}{2}}\frac{(\mathtt{dzt})_{i,j,k-\frac{1}{2}}}{2}. \tag{7.34}$$

b. Discretization of the geopotential term

The geopotential term is also discretized so that a round-off error is minimized. Considering that the time-dependent part of the actual depth $z=z(s)$ is due to the perturbation ($z'(s)$) from the state of rest ($z_0(s)$) caused by the sea level variation, taking differentiation for $z(s)$ at depth is not quite accurate owing to the numerical round-off. Then we separate the actual depth as $z(s)=z_0(s)+z'(s)$ and only use $z'(s)$ for horizontal gradient of geopotential, that is,

$$\frac{g\rho'}{\rho_0}\nabla_s z=\frac{g\rho'}{\rho_0}\nabla_s z'(s). \tag{7.35}$$

Here, we used the fact that the depth of the constant s-surface is flat at the state of rest, i.e. $\nabla_s z_0(s)=0$. (Again, we cannot use this simplicity for the bottom boundary layer. See Chapter 16 for details.) Then, the term is differentiated as

$$\begin{aligned}&\left[\frac{g\rho'}{\rho_0}\nabla_s z'\right]_{i+\frac{1}{2},j+\frac{1}{2}}\\ &=\frac{g}{\rho_0}\left\{\left[\frac{\frac{\rho'_{i+1,j}+\rho'_{i,j}}{2}\frac{z'_{i+1,j}-z'_{i,j}}{\Delta x_{i+\frac{1}{2},j}}+\frac{\rho'_{i+1,j+1}+\rho'_{i,j+1}}{2}\frac{z'_{i+1,j+1}-z'_{i,j+1}}{\Delta x_{i+\frac{1}{2},j+1}}}{2}\hat{\mathbf{x}}\right]+\left[\frac{\frac{\rho'_{i,j+1}+\rho'_{i,j}}{2}\frac{z'_{i,j+1}-z'_{i,j}}{\Delta y_{i,j+\frac{1}{2}}}+\frac{\rho'_{i+1,j+1}+\rho'_{i+1,j}}{2}\frac{z'_{i+1,j+1}-z'_{i+1,j}}{\Delta y_{i+1,j+\frac{1}{2}}}}{2}\hat{\mathbf{y}}\right]\right\}.\end{aligned} \tag{7.36}$$

Here, we follow the expression presented in Section 3.3.1 of the reference manual of GFDL-MOM.

c. The sea-floor grid (except for bottom boundary layer)

Owing to the introduction of the partial cell, the grid width of the bottom U-cell may depend on the horizontal position. The pressure gradient term in (7.28) is the gradient of pressure on constant $s(z^*)$-surface. Thus, the pressure gradient force on a partial U-cell is evaluated using the pressure perturbation p' obtained by integrating to the depth where velocity is defined on z^* coordinate (the central depth of the bottom U-cell). These are the points with triangle (△) symbols in Figure 3.5.

To calculate the pressure gradient, the actual depth of the vertical level where velocity is defined for the bottom U-cell ($s = s^U_{k=kbtm}$) must be obtained at all four corner T-points of a U-cell. Here, these are determined using the ratio of the half width of a U-cell $\frac{1}{2}\Delta s^U$ to the width of a T-cell Δs^T:

$$z^U_{kbtm} = z^T_{kbtm-1} - \Delta z^T_{kbtm} \frac{\Delta s^U_{kbtm}}{2\Delta s^T_{kbtm}}. \tag{7.37}$$

The depth anomaly used for computing geopotential gradient anomaly may be obtained in the same way:

$$z'^U_{kbtm} = z'^T_{kbtm-1} - \Delta z'^T_{kbtm} \frac{\Delta s^U_{kbtm}}{2\Delta s^T_{kbtm}}. \tag{7.38}$$

The finite difference expression for horizontal gradient is formally the same as (7.33) and (7.36). However, the vertical integration to obtain p' is performed to the depth where velocity is defined for the bottom U-cell. Geopotential term is evaluated using a depth anomaly of $s(z^*)$-surface. Thus, on the same vertical level, the algorism is different depending on whether it is bottom cell or not.

7.3 Viscosity

The viscosity in an ocean general circulation model seeks to attenuate numerical noise rather than parameterizing the subgrid-scale momentum transport. The momentum advection scheme should conserve the total kinetic energy in the general three-dimensional flows and the total enstrophy in the two-dimensional flows. Therefore, spatially and temporally centered discretization should be used, although this inevitably produces near-grid-size noise accompanying numerical dispersion. In eddy-resolving models, the current velocity and the numerical noise are greater than those of eddy-less models. A biharmonic viscosity scheme has been widely used to reduce numerical noise while maintaining the eddy structure.

The viscosity term is represented by $\mathcal{V}$ and is calculated separately in the lateral and vertical directions, i.e., the fourth and fifth terms, respectively, on the r.h.s. of (7.1) and (7.2). For horizontal viscosity, the harmonic (default) or biharmonic (`VISBIHARM` option) scheme can be selected. Anisotropy of viscosity with respect to the flow direction can be applied (`VISANISO` option) when harmonic viscosity is chosen. The viscosity coefficient is a constant by default but can be determined as a function of local velocity gradients and grid-size (`SMAGOR` option).

For vertical viscosity, the harmonic scheme is used and the local coefficient is the larger one of the background constant and the value calculated from a turbulence closure scheme. A parameterization of bottom friction (Weatherly et al., 1980) is adopted at the lowest layer.

7.3.1 Horizontal viscosity

The specific form for harmonic viscosity is shown here. Horizontal tension D_T and shear D_S are defined as follows:

$$D_T = h_\psi \frac{\partial}{h_\mu \partial \mu}\left(\frac{u}{h_\psi}\right) - h_\mu \frac{\partial}{h_\psi \partial \psi}\left(\frac{v}{h_\mu}\right), \tag{7.39}$$

$$D_S = h_\psi \frac{\partial}{h_\mu \partial \mu}\left(\frac{v}{h_\psi}\right) + h_\mu \frac{\partial}{h_\psi \partial \psi}\left(\frac{u}{h_\mu}\right). \tag{7.40}$$

The viscosity terms are

$$\mathcal{V}_u = \frac{1}{h_\psi^2} \frac{\partial}{h_\mu \partial \mu}\left(h_\psi^2 \sigma_T\right) + \frac{1}{h_\mu^2} \frac{\partial}{h_\psi \partial \psi}\left(h_\mu^2 \sigma_S\right), \tag{7.41}$$

$$\mathcal{V}_v = \frac{1}{h_\psi^2} \frac{\partial}{h_\mu \partial \mu}\left(h_\psi^2 \sigma_S\right) - \frac{1}{h_\mu^2} \frac{\partial}{h_\psi \partial \psi}\left(h_\mu^2 \sigma_T\right), \tag{7.42}$$

where $\sigma_T = \nu_H D_T$ and $\sigma_S = \nu_H D_S$, and ν_H is the horizontal viscosity coefficient. The above representation of the viscous term was derived by Bryan (1969) and is consistent with Smagorinsky (1963).

If we take $h_\mu = 1$, $h_\psi = 1$, the coordinate system is Cartesian. In this case, the viscosity term is reduced to the Laplacian form if the viscosity coefficient is a constant. In the geographic coordinate system, where $(\mu, \psi) = (\lambda, \phi)$, $h_\lambda = a\cos\phi$, and $h_\phi = a$, tension and shear are

$$D_T = \frac{1}{a\cos\phi}\frac{\partial u}{\partial\lambda} - \frac{1}{a}\frac{\partial v}{\partial\phi} - \frac{v}{a}\tan\phi, \tag{7.43}$$

$$D_S = \frac{1}{a\cos\phi}\frac{\partial v}{\partial\lambda} + \frac{1}{a}\frac{\partial u}{\partial\phi} + \frac{u}{a}\tan\phi. \tag{7.44}$$

The viscosity terms in this case are

$$\mathcal{V}_u = \frac{1}{a\cos\phi}\frac{\partial}{\partial\lambda}\sigma_T + \frac{1}{a}\frac{\partial}{\partial\phi}\sigma_S - \sigma_S\frac{2\tan\phi}{a}, \tag{7.45}$$

$$\mathcal{V}_v = \frac{1}{a\cos\phi}\frac{\partial}{\partial\lambda}\sigma_S - \frac{1}{a}\frac{\partial}{\partial\phi}\sigma_T + \sigma_T\frac{2\tan\phi}{a}, \tag{7.46}$$

where the third term on the r.h.s. is called the metric term.

When biharmonic viscosity is used (`VISBIHARM` option), the above operation is repeated twice using a viscosity coefficient ν_{BH}. The terms $\mathcal{V}_u$ and $\mathcal{V}_v$ given by (7.41) and (7.42) are sign-reversed and substituted as u and v in equations (7.39) and (7.40). A biharmonic scheme dissipates noise only on scales near the grid size. This scale selectivity allows the explicitly represented eddies to survive without unphysical damping in eddy-resolving models, although we must note that a biharmonic operator produces overshootings and spurious oscillations of variables (Delhez and Deleersnijder, 2007). A biharmonic viscosity scheme is not suitable for coarse resolution models that cannot resolve mesoscale eddies.

A non-slip condition is used for the side boundaries of topography by default in MRI.COM. A free-slip condition assuming zero viscosity there is also available.

7.3.2 Horizontal anisotropic viscosity (`VISANISO`)

Smith and McWilliams (2003) proposed a method of making a harmonic viscosity scheme anisotropic in an arbitrary direction. Setting σ_T and σ_S in equations (7.41) and (7.42) to

$$\begin{pmatrix} \sigma_T \\ \sigma_S \end{pmatrix} = \left[\begin{pmatrix} \frac{1}{2}(\nu_0 + \nu_1) & 0 \\ 0 & \nu_1 \end{pmatrix} + (\nu_0 - \nu_1) n_\mu n_\psi \begin{pmatrix} -2n_\mu n_\psi & n_\mu^2 - n_\psi^2 \\ n_\mu^2 - n_\psi^2 & 2n_\mu n_\psi \end{pmatrix} \right] \begin{pmatrix} D_T \\ D_S \end{pmatrix}, \tag{7.47}$$

where $\hat{\mathbf{n}} = (n_\mu, n_\psi)$ is a unit vector in an arbitrary direction and ν_0 (ν_1) is the viscosity coefficient parallel (perpendicular) to $\hat{\mathbf{n}}$. When `VISANISO` option is selected, $\hat{\mathbf{n}}$ is set to the direction of local flow in MRI.COM. Given the harmonic viscosity only in the direction of flow ($\nu_1 = 0$), the numerical noise is erased while the swift currents and eddy structures are maintained.

The following is a note on usage. The behavior of this scheme is specified at run time by namelist `nml_visaniso` (Table 7.2). The ratio ν_1/ν_0 should be given by `cc0` (default value is 0.2). The ratio at the lateral boundary should be given by `cc1` (default value is 0.5). When the variable `flgvisequator` is set as a positive number in the namelist, the ratio ν_1/ν_0 is tapered linearly from `cc0` at the latitude `flgvisequator` (in degrees) to `vis_factor_equator` at the Equator. The ratio is not tapered when a negative number is set, and the default value of `flgvisequator` is -1.

Table7.2 Namelist `nml_visaniso` anisotropic horizontal viscosity

variable	units	description	usage
`cc0`	1	the factor of anisotropy in viscosity; perpendicular / parallel (ν_1/ν_0) to the flow	default = 0.2
`cc1`	1	the factor (ν_1/ν_0) at lateral boundary	default = 0.5
`figvisequator`	degree latitude	the factor is tapered toward the Equator; when |LAT| < `flgvisequator` [deg]	default = -1 (no tapering)
`vis_factor_equator`	1	the factor at Equator when `flgvisequator` > 0	default = 0.0

7.3.3 Smagorinsky parameterization for horizontal viscosity (SMAGOR option)

To give the necessary but minimum viscosity to reduce numerical noise, the viscosity coefficient is made proportional to the local deformation rate (SMAGOR option; Smagorinsky, 1963; Griffies and Hallberg, 2000). When this parameterization is used with the biharmonic scheme, the scale selectivity of the viscosity scheme becomes more effective.

Defining deformation rate $|D|$:

$$|D| = \sqrt{D_T^2 + D_S^2}, \tag{7.48}$$

the viscosity coefficients are set as follows:

$$\nu_H = \left(\frac{C\Delta_{\min}}{\pi}\right)^2 |D|, \tag{7.49}$$

$$\nu_{BH} = \frac{\Delta_{\min}^2}{8}\nu_H, \tag{7.50}$$

where C (smagor_scale) is a dimensionless scaling parameter set by considering numerical stability and $\Delta_{\min}$ is the smaller of the zonal and meridional grid widths.

The parameter C should be selected to satisfy the following conditions.

- Restriction of grid Reynolds number:

$$\nu_H > U\frac{\Delta_{\min}}{2}, \tag{7.51}$$

- Restriction on the width of the lateral boundary layer:

$$\nu_H > \beta\Delta_{\min}^3, \tag{7.52}$$

- CFL condition:

$$\nu_H < \frac{\Delta_{\min}^2}{2\Delta t}, \tag{7.53}$$

where $\beta = df/dy$ is the meridional gradient of the Coriolis parameter. Scaling the deformation rate $|D|$ by $U/\Delta_{\min}$ gives the condition for stability: $C > \pi/\sqrt{2} \approx 2.2$ from (7.51) (Griffies and Hallberg, 2000).

Behavior of this scheme at run time is specified by namelist nml_smagor, whose components are listed on Table 7.3.

Table7.3 Namelist nml_smagor for Smagorinsky parameterization of horizontal viscosity coefficient

variable	units	description	usage
smagor_scale	1	scaling factor coefficient	default = −1.0
smagor_diff_ratio	1	ratio for diffusivity to scaling factor of viscosity	default = −1.0
l_smagor_nonzero_bg	logical	Use background viscosity as given by nml_baroclinic_visc_horz (Table 7.4)	default = .false.

7.3.4 Discretization of the horizontal viscosity term

Using the notations

$$\delta_\mu A_{i,j} \equiv \frac{A_{i+\frac{1}{2},j} - A_{i-\frac{1}{2},j}}{\Delta\mu}, \quad \delta_\psi A_{i,j} \equiv \frac{A_{i,j+\frac{1}{2}} - A_{i,j-\frac{1}{2}}}{\Delta\psi},$$
$$\delta_i A_{i,j} \equiv A_{i+\frac{1}{2},j} - A_{i-\frac{1}{2},j}, \quad \delta_j A_{i,j} \equiv A_{i,j+\frac{1}{2}} - A_{i,j-\frac{1}{2}},$$

and

$$\overline{A_{i,j}}^{\mu} \equiv \frac{1}{2}(A_{i-\frac{1}{2},j} + A_{i+\frac{1}{2},j}), \quad \overline{A_{i,j}}^{\psi} \equiv \frac{1}{2}(A_{i,j-\frac{1}{2}} + A_{i,j+\frac{1}{2}}),$$

deformation rates are discretized as follows:

$$
\begin{aligned}
D_{T\,i,j} &= \frac{h_{\psi i,j}}{h_{\mu i,j}} \overline{\delta_\mu \left(\frac{u}{h_\psi}\right)_{i,j}}^{\psi} - \frac{h_{\mu i,j}}{h_{\psi i,j}} \overline{\delta_\psi \left(\frac{v}{h_\mu}\right)_{i,j}}^{\mu}, \\
D_{S\,i,j} &= \frac{h_{\psi i,j}}{h_{\mu i,j}} \overline{\delta_\mu \left(\frac{v}{h_\psi}\right)_{i,j}}^{\psi} + \frac{h_{\mu i,j}}{h_{\psi i,j}} \overline{\delta_\psi \left(\frac{u}{h_\mu}\right)_{i,j}}^{\mu}.
\end{aligned} \tag{7.54}
$$

Horizontal viscosity forces of (7.41) and (7.42) are discretized as follows:

$$
\begin{aligned}
F_{x\,i+\frac{1}{2},j+\frac{1}{2}} &= \frac{1}{\Delta V_{i+\frac{1}{2},j+\frac{1}{2}}} \\
&\times \left[\frac{1}{h^2_{\psi i+\frac{1}{2},j+\frac{1}{2}}} \delta_i \left(\Delta y \Delta z h_\psi^2 \overline{\nu_H D_T}^{\psi}\right)_{i+\frac{1}{2},j+\frac{1}{2}} + \frac{1}{h_{\mu}{}^2_{i+\frac{1}{2},j+\frac{1}{2}}} \delta_j \left(\Delta x \Delta z h_\mu^2 \overline{\nu_H D_S}^{\mu}\right)_{i+\frac{1}{2},j+\frac{1}{2}} \right], \\
F_{y\,i+\frac{1}{2},j+\frac{1}{2}} &= \frac{1}{\Delta V_{i+\frac{1}{2},j+\frac{1}{2}}} \\
&\times \left[\frac{1}{h^2_{\psi i+\frac{1}{2},j+\frac{1}{2}}} \delta_i \left(\Delta y \Delta z h_\psi^2 \overline{\nu_H D_S}^{\psi}\right)_{i+\frac{1}{2},j+\frac{1}{2}} - \frac{1}{h_{\mu}{}^2_{i+\frac{1}{2},j+\frac{1}{2}}} \delta_j \left(\Delta x \Delta z h_\mu^2 \overline{\nu_H D_T}^{\mu}\right)_{i+\frac{1}{2},j+\frac{1}{2}} \right].
\end{aligned} \tag{7.55}
$$

The non-slip condition at the side boundaries of topography is discretized as follows. When the grid point $(i-\frac{1}{2}, j+\frac{1}{2})$ is defined as a (vertically partial) land (Figure 7.7a), the velocity gradients at the wall are calculated as follows:

$$
\begin{aligned}
\left(\frac{\partial u}{\partial x}\right)_{i,j+\frac{1}{2}} &= \frac{u_{i+\frac{1}{2},j+\frac{1}{2}}}{\Delta x^-_{ij}}, \\
\left(\frac{\partial v}{\partial x}\right)_{i,j+\frac{1}{2}} &= \frac{v_{i+\frac{1}{2},j+\frac{1}{2}}}{\Delta x^-_{ij}},
\end{aligned} \tag{7.56}
$$

where Δx^-_{ij} is the length between the points $(i, j+\frac{1}{2})$ and $(i+\frac{1}{2}, j+\frac{1}{2})$. The contribution of this wall to the force is:

$$
\begin{aligned}
F^W_{x\;i+\frac{1}{2},j+\frac{1}{2}} &= -\frac{1}{\Delta V_{i+\frac{1}{2},j+\frac{1}{2}} h_{\psi}{}^2_{i+\frac{1}{2},j+\frac{1}{2}}} \Delta y_{i,j+\frac{1}{2}} \Delta \tilde{z}_{i,j+\frac{1}{2}} h_{\psi}{}^2_{i-\frac{1}{2},j} \nu_{H i-\frac{1}{2},j} \frac{u_{i+\frac{1}{2},j+\frac{1}{2}}}{\Delta x^-_{i+\frac{1}{2},j+\frac{1}{2}}}, \\
F^W_{y\;i+\frac{1}{2},j+\frac{1}{2}} &= -\frac{1}{\Delta V_{i+\frac{1}{2},j+\frac{1}{2}} h_{\psi}{}^2_{i+\frac{1}{2},j+\frac{1}{2}}} \Delta y_{i,j+\frac{1}{2}} \Delta \tilde{z}_{i,j+\frac{1}{2}} h_{\psi}{}^2_{i-\frac{1}{2},j} \nu_{H i-\frac{1}{2},j} \frac{v_{i+\frac{1}{2},j+\frac{1}{2}}}{\Delta x^-_{i+\frac{1}{2},j+\frac{1}{2}}},
\end{aligned} \tag{7.57}
$$

where $\Delta \tilde{z}_{i,j+\frac{1}{2}}$ is the wall height.

7.3.5 Vertical viscosity

Only the harmonic scheme is considered. The vertical momentum flux is assumed to be proportional to the vertical gradient of velocity. For the upper part of a U-cell at the $(k-\frac{1}{2})$th vertical level, the momentum flux (positive upward) is calculated as follows:

$$
-\left(\nu_v \frac{\partial u}{\partial z}\right)_{k-1} = -\nu_{v\,k-1} \frac{u_{k-\frac{3}{2}} - u_{k-\frac{1}{2}}}{\Delta z_{k-1}},
$$

where $\Delta z_{k-1} = (\Delta z_{k-\frac{3}{2}} + \Delta z_{k-\frac{1}{2}})/2$, $\Delta z_{k-\frac{1}{2}}$ is the thickness of the U-cell (dzu), and ν_v is the vertical viscosity coefficient. Similarly, the momentum flux in the lower part of the U-cell is calculated as follows:

$$
-\left(\nu_v \frac{\partial u}{\partial z}\right)_{k} = -\nu_{v\,k} \frac{u_{k-\frac{1}{2}} - u_{k+\frac{1}{2}}}{\Delta z_{k}},
$$

where $\nu_{v\,k}$ is set to zero if the $(k+\frac{1}{2})$th level is the solid Earth. The bottom friction is calculated independently (see the next subsection). Also note that the variations of the grid thickness due to the partial bottom cell and the undulation of the sea surface are not considered when evaluating fluxes for simplicity.

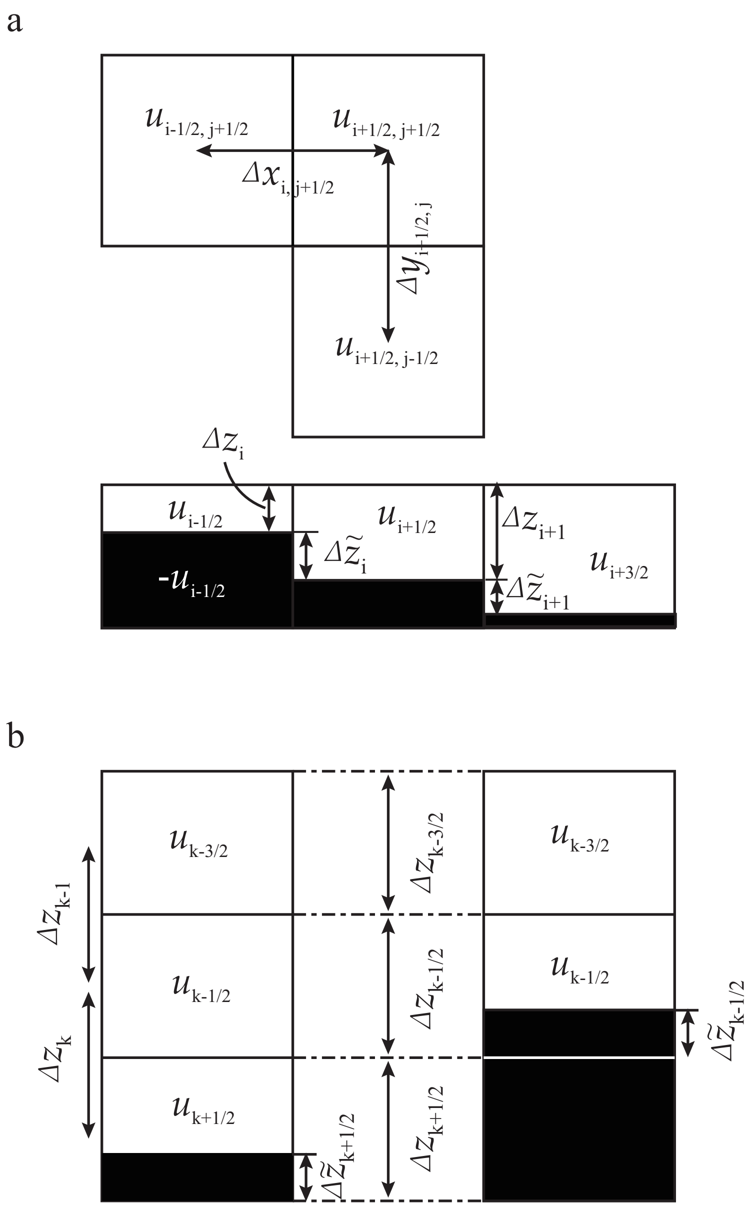

Figure7.7 (a) A schematic distribution of grids for horizontal viscosity. Upper: Plan view. Lower: Side view. The shadings denote solid earth. (b) A schematic distribution of grids for vertical viscosity. Side views. Left: The lower adjacent layer ($k+\frac{1}{2}$) has a sea bed. Right: The U-cell ($k-\frac{1}{2}$) has a sea bed.

To calculate viscosity, the divergence of the momentum flux is first calculated. The expression for the vertical viscosity term is

$$\frac{\partial}{\partial z}\left(\nu_v \frac{\partial u}{\partial z}\right)_{k-\frac{1}{2}} = \frac{(\nu_v \frac{\partial u}{\partial z})_{k-1} - (\nu_v \frac{\partial u}{\partial z})_k}{\widehat{\Delta z}_{k-\frac{1}{2}}} = \frac{\nu_{v\,k-1}(u_{k-\frac{3}{2}} - u_{k-\frac{1}{2}})}{\Delta z_{k-1}\widehat{\Delta z}_{k-\frac{1}{2}}} - \frac{\nu_{v\,k}(u_{k-\frac{1}{2}} - u_{k+\frac{1}{2}})}{\Delta z_k \widehat{\Delta z}_{k-\frac{1}{2}}} \tag{7.58}$$

where the variation of the grid thickness for the U-cell due to the partial bottom cell is now taken into account and is represented by $\widehat{\Delta z}$, that is, $\widehat{\Delta z}_{k-\frac{1}{2}} = \Delta z_{k-\frac{1}{2}} - \widetilde{\Delta z}_{k-\frac{1}{2}}$ (Figure 7.7(b)). Note that the first term on the r.h.s. of equation (7.58) is set to zero in calculating the viscosity term for the vertical level of $\frac{1}{2}$ ($k = 1$). See section 14.1 for sea surface wind stress. For the vertical viscosity coefficient ν_v, MRI.COM uses the larger of the value predicted by a turbulent closure scheme and a background one.

7.3.6 Bottom friction

When a U-cell in the $(k-\frac{1}{2})$th layer contains solid earth (Figure 7.7(b) right), the stress from the lower boundary (τ_x^b, τ_y^b) is calculated following Weatherly et al. (1980). The specific expression is as follows:

$$\begin{pmatrix} \tau_x^b \\ \tau_y^b \end{pmatrix} = -\rho_0 C_{\mathrm{btm}} \sqrt{u_{k-\frac{1}{2}}^2 + v_{k-\frac{1}{2}}^2} \begin{pmatrix} \cos\theta_0 & -\sin\theta_0 \\ \sin\theta_0 & \cos\theta_0 \end{pmatrix} \begin{pmatrix} u_{k-\frac{1}{2}} \\ v_{k-\frac{1}{2}} \end{pmatrix},$$

where C_{btm} is a dimensionless constant. Viscous stress at the lower boundary has a magnitude proportional to the square of the flow speed at the U-cell and an angle $(\theta_0 + \pi)$ relative to the flow direction.

In MRI.COM,

$$\begin{aligned} C_{\mathrm{btm}} &= 1.225 \times 10^{-3} \\ \theta_0 &= \pm\pi/18 \quad \mathrm{rad} \qquad (\equiv\ 10^\circ), \end{aligned}$$

where θ_0 is positive (negative) in the northern (southern) hemisphere. The variables are designated in the model as C_{btm} = `abtm`, $\cos\theta_0$ = `bcs`, and $\sin(\pm\theta_0)$ = `isgn` $*$ `bsn`, where `isgn` = 1 in the northern hemisphere and `isgn` = −1 in the southern hemisphere.

7.4 Coriolis term

Because MRI.COM employs Arakawa B-grid arrangement, both of the horizontal components of velocity are defined at the same point. Coriolis term is evaluated by using the middle time level for the leap-frog scheme and the start time level for the Euler-backward scheme.

7.5 Usage

Runtime behavior of the baroclinic mode in the default settings is specified by the five namelist blocks (some of them are optional) shown on Tables 7.4 through 7.8. For the initial condition of the 3D velocity field, restart file must be prepared for X- and Y-ward velocities.

In addition, following model options are available.

`BIHARMONIC` or `VISBIHARM`: Biharmonic horizontal viscosity is used instead of harmonic viscosity
Specify `visc_horz_cm4ps` [cm^{4}sec^{-1}] instead of `visc_horz_cm2ps` [cm^{2}sec^{-1}] in namelist `nml_baroclinic_visc_horz`. See Section 7.3.1 for detail.

`VISANISO`: Anisotropic viscosity coefficients are used
Specify the coefficients by `nml_visaniso` (Table 7.2). See Section 7.3.2 for detail.

`SMAGOR` or `SMAGHD`: Smagorinsky parameterization is used for horizontal viscosity
Specify `nml_smagor` (Table 7.3) for factors of the Smagorinsky parameterization. See Section 7.3.3 for detail.

`VIS9P`: Nine points are used in computing viscosity
Five points are used by default.

See `docs/README.Namelist` for namelist details.

Table7.4 Namelist `nml_baroclinic_visc_horz` (required) for the horizontal viscosity (see Section 7.5)

variable	units	description	usage
`visc_horz_cm2ps`	cm^2 sec^{-1}	horizontal viscosity (ν_H in Section 7.3.1)	required

Continued on next page

Table 7.4 – continued from previous page

variable	units	description	usage
file_visc_horz_2d	$cm^2\ sec^{-1}$	2D distribution of viscosity	optional (This overwrites visc_horz_cm2ps.)
slip_factor	factor	0.d0 means no-slip condition, while 1.d0 slip (Section 7.3.1)	default = 0.d0 (only valid with VIS9P option)

Table7.5 Namelist nml_visc_vert_bg (optional) for vertical viscosity (see Section 7.5)

variable	units	description	usage
visc_vert_bg_cm2ps	$cm^2\ sec^{-1}$	background vertical viscosity (ν_v in Section 7.3.5)	default = 1.d0

Table7.6 Namelist nml_bottom_friction (optional) for the bottom friction (see Section 7.5)

variable	units	description	usage
btmfrc_scale	1	C_{btm} in Section 7.3.6	default = 1.225d−3
btmfrc_angle_deg	degree	θ_0	default = 1.d1
file_btm_frc_2d	file name	2D distribution of C_{btm}	optional (This overwrites btmfrc_scale)

Table7.7 Namelist nml_hvisc_add (optional) for additional horizonta viscosity (see Section 7.5)

variable	units	description	usage
l_hvisc_add_harmonic	logical	use additional harmonic viscosity or not	default = .false.
file_hvisc_harmonic	$cm^2\ sec^{-1}$	2D distribution of viscosity	file name

Table7.8 Namelist nml_baroclinic_run (optional) for starting the baroclinic mode (see Section 7.5)

variable	units	description	usage
l_rst_baroclinic_in	logical	read initial restart for 3D velocity or not	default = l_rst_in